

Elsevier required licence: ©2023. This manuscript version is made available under the CC-BY-NC-ND 4.0 license <http://creativecommons.org/licenses/by-nc-nd/4.0/>

The definitive publisher version is available online at

<https://doi.org/10.1016/j.scitotenv.2023.163901>

Desalination by the Forward Osmosis: advancement and Challenges

Nada Abounahia¹, Ibrar Ibrar², Tayma Kazwini², Ali Altaee^{2*}, Akshaya K. Samal³, Syed Javaid Zaidi^{1*}, Alaa H. Hawari^{4*}

¹UNESCO Chair for Desalination and Water Treatment, Center for Advanced Materials (CAM), Qatar University, Doha, Qatar

²Centre for Green Technology, School of Civil and Environmental Engineering, the University of Technology Sydney, 15 Broadway, NSW, 2007, Australia

³Centre for Nano and Material Sciences, Jain University, Jain Global Campus, Ramanagara, Bangalore 562112, India

⁴Department of Civil and Architectural Engineering, College of Engineering, Qatar University, PO Box 2713, Doha, Qatar

*Corresponding author email address: ali.altaee@uts.edu.au

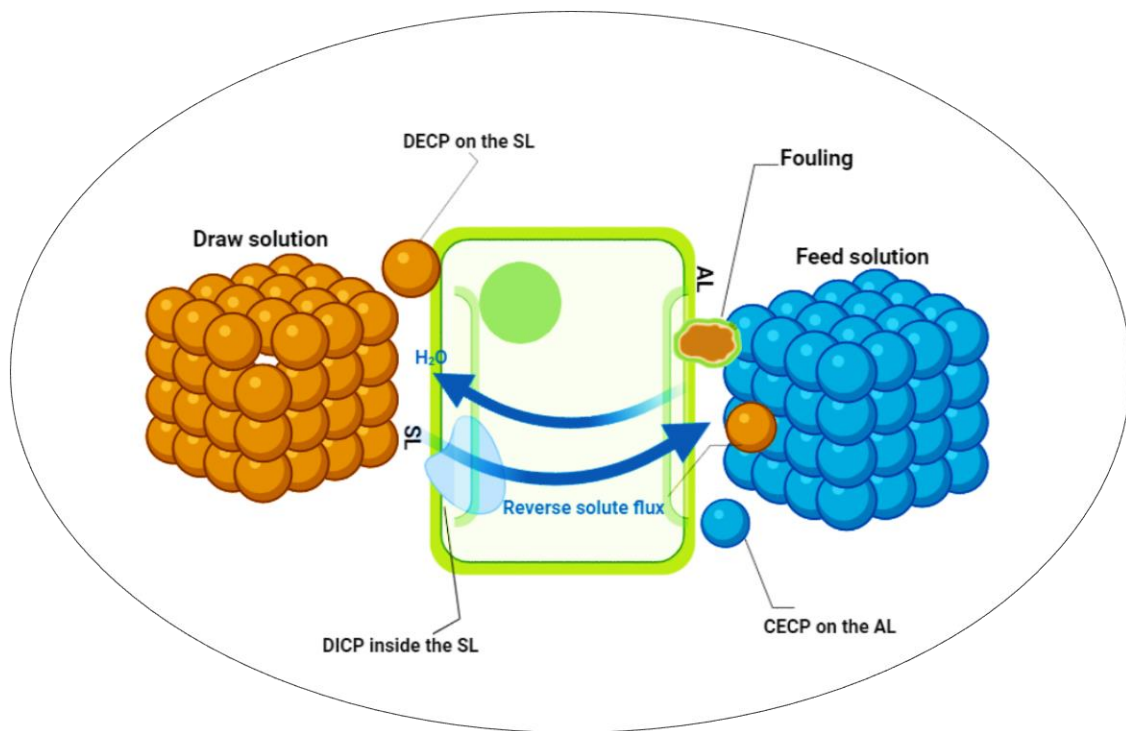
*Corresponding author's phone number: +61295149668

Abstract.

Forward osmosis (FO) has become a promising membrane technology for desalination and water treatment due to its simplicity, low energy consumption, and low fouling tendency compared to pressure-driven membrane processes. Therefore, the advancement in FO process modelling was one of the main objectives of this paper. On the other hand, the membrane characteristics and draw solute type represent the main FO process factors determining its technical performance and economical perspectives. Thus, this review mainly highlights the commercially available FO membrane characteristics and the development of lab-scale fabricated membranes based on cellulose triacetate and thin-film nanocomposite membranes. These membranes were discussed by considering their fabrication and modification techniques. Additionally, the novelty of different draw agents and their effects on FO performance have

been analyzed in this study. Moreover, the review touched upon different pilot-scale studies on the FO process. Finally, this paper has stated the overall FO process advances along with its drawbacks. This review is anticipated to benefit the research and desalination scientific community by having an overview of the major FO components that require additional attention and development.

Keywords: Forward Osmosis, Draw Solution, Membranes, Separation, Desalination



Graphical Illustration

1. Introduction:

Membrane processes are the most common purification and separation technology for fresh water supply (Yadav et al., 2020c). The high recovery rate and salt rejection of reverse osmosis (RO) and Nanofiltration (NF) membranes are distinctive features of membrane technologies which make them competitive with other technologies such as thermal desalination (Ibrar et al., 2020a). Pressure-driven membrane technology, such as RO and NF membranes, are suitable for desalinating a wide range of saline solutions, including seawater, groundwater, and

wastewater. The specific power consumption for desalinating brackish water of 1.5 g/L TDS is about 0.5 kWh/m³ (M. A. Hafiz et al., 2021). In contrast, for seawater desalination, the specific power consumption of the RO, including the pre-treatment energy, is slightly over 4 kWh/m³ (Kim et al., 2019). Despite the advantages of pressure-driven membrane technology, it suffers inherited drawbacks, including membrane fouling and relatively high desalination energy requirements.

To overcome conventional RO drawbacks, forward osmosis (FO) technology was suggested for seawater desalination (Aende et al., 2020). The FO process operates by the osmotic pressure difference across a semipermeable membrane; hence, membrane fouling accelerated by the hydraulic pressure is minimized (Chun et al., 2017). The process flexibly accommodates a wide range of draw solution types, including organic, inorganic, magnetically coated particles, ionic liquid and many other draw solutions to combine with the feed solution (Long et al., 2018). The product of the FO process is merely a concentrated draw solution that requires further treatment before use. Regeneration of the draw solution also becomes an issue because it is the most expensive and energy requirement step in the FO process, despite that regeneration is not required in a few applications (Aende et al., 2020). Thermal and membrane processes are the main technologies for regenerating the draw solution, but other technologies, such as the magnetic separation process, were suggested to regenerate magnetic draw solutions (Hafiz et al., 2022). Selecting the regeneration process for a draw solution is also dictated by the type of draw solution to reduce energy consumption. For example, although thermolytic draw solutions are suitable for regeneration by thermal or membrane technologies, thermal technologies are more cost-effective (Altaee et al., 2018).

The membrane is the other key component in the FO process that should be designed to special specifications to meet the requirements for the membrane to have a thin structure parameter (Kahrizi et al., 2022). Commercial membranes are currently available for the FO process in

different materials and configurations (Li et al., 2020). However, fouling and concentration polarization (CP) are inevitable phenomena in the FO process that should be addressed in the design of the FO membrane. Experimentally, CP is more severe when the draw solution faces the membrane support layer due to the complexity of mitigating its effect (Kahrizi et al., 2022; Suzaimi et al., 2020). It is also found that membrane fouling would be easier to mitigate when the draw solution faces the support layer, especially when using an impaired-quality feed solution (Lee et al., 2020). As such, researchers developed myriad methods to mitigate the impact of fouling on the performance of the FO membrane (Chun et al., 2017).

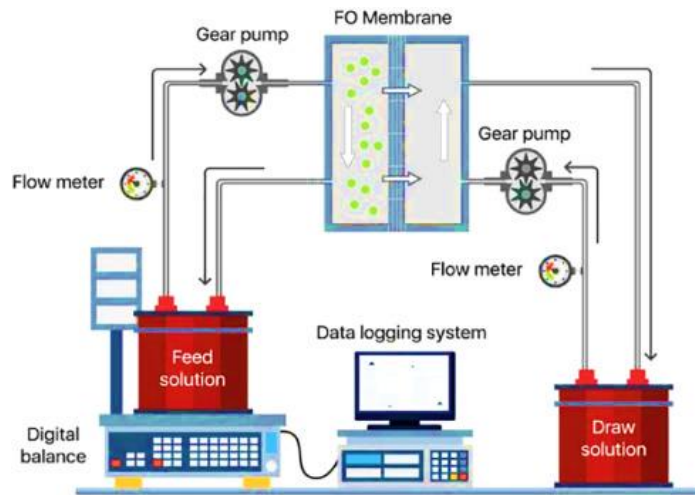
The FO membrane and draw solution, the main component of the FO process, were over-searched in the last two decades to understand their impacts and optimize the performance of the FO process. Despite the many successes in membrane fabrications and novel draw solution developments over time, the way for the FO process to be fully commercialized needs more work due to our hindsight to understand the process's precise design and operation requirements. This study will cover the main achievements in the FO process and provide an overview of the aspects that requires more attention and development. The advancement in process modelling and machine learning to predict the FO process performance was reviewed to highlight the importance of applying artificial intelligence technology in the membrane processes. The study also provided an update on the fabrication of FO membranes in commercial and laboratory-made membranes to compare their performances and impediments challenging the commercialization of laboratory-made membranes. The other key factor in the FO process that was touched upon in this study is the draw solution and how it affects the process performance. Finally, the study reviewed the FO pilot plant tests in the last 2 decades to provide insight into the process's major achievements.

2. FO modelling

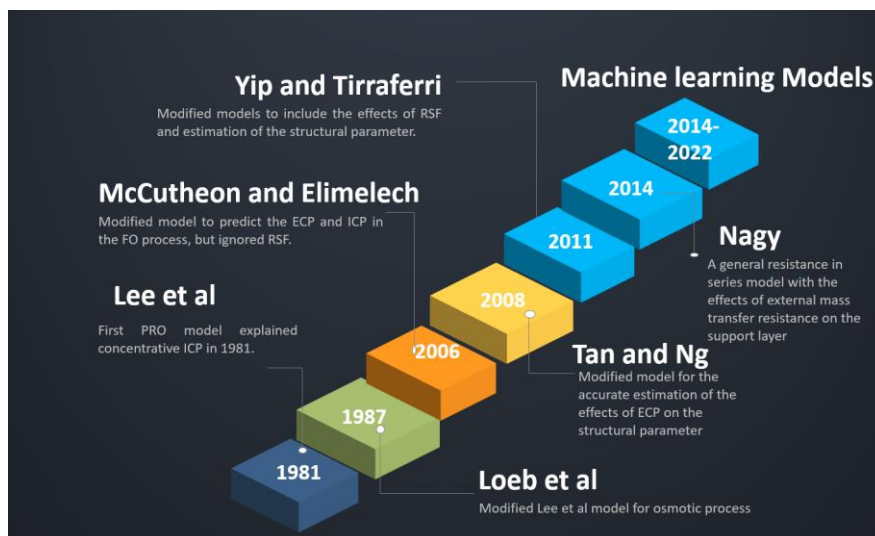
Forward osmosis or FO process is based on water transport across a semipermeable membrane from a solution of low osmotic pressure (feed solution or FS) to a solution of high osmotic pressure (draw solution or DS). **Figure 1a** presents a schematic of the forward osmosis crossflow lab-scale filtration system. Two pumps are used to circulate the feed and draw solutions. The flow rate of the feed and draw solutions is measured through flowmeters. The FO process has emerged as a possible alternative to other membrane-based technologies for wastewater treatment and seawater desalination due to its low fouling propensity and the need for external hydraulic pressure (Rodríguez-Alegre et al., 2023). However, unlike other membrane separation processes such as reverse osmosis and nanofiltration, the FO process suffers from external and internal concentration polarisation, the latter only inherent to the FO process. Accurate assessment and measurement of concentration polarisation are vital for an efficient FO operation. Therefore, proper accounting of mass transfer across the forward osmosis membrane is critical to improve the forward osmosis membrane performance and for the forward osmosis process to compete against other commercial technologies such as RO and NF. The fundamental Equation of water flux J_w across a membrane is given by Equation (1) (Ibrar et al., 2022c).

$$J_w = A\Delta\pi - \Delta P \quad (1)$$

where $\Delta\pi$ represents the osmotic pressure difference across the membrane, and ΔP is the hydraulic pressure which is zero in the FO process since it operates without hydraulic pressures. Equation (1), however, is not practical and does not simulate the water flux across a FO process since the effects of internal concentration polarisation are ignored. Lee et al. (1981) presented the first model for water flux prediction in pressure-retarded osmosis (PRO), considering the effect of concentration polarisation. The model has been revised and has seen many improvements by several researchers over time, as presented in **Figure 1b**.



(a)



(b)

Figure 1: Forward osmosis lab setup and models, a) Forward osmosis lab-scale experimental setup, and b) FO flux model's timeline from 1981-2022 shows the most prominent in the literature.

McCutcheon and Elimelech₍₂₀₀₆₎ extended the model of Lee et al. (1981) by incorporating the effects of external and internal concentration polarisation on flux behaviour. According to the study, water flux in the FO process operating in the PRO mode (active membrane layer faces the draw solution) is given by Equation (2).

$$J_w^{PRO} = A \left[\pi_{D,b} \exp\left(-\frac{J_w}{k}\right) - \pi_{F,b} \exp(J_w K) \right] \quad (2)$$

For the FO membrane operating in the FO mode (active membrane layer faces the feed solution), water flux is given by Equation 3.

$$J_w^{FO} = A \left[\pi_{D,b} \exp(J_w K) - \pi_{F,b} \exp\left(-\frac{J_w}{k}\right) \right] \quad (3)$$

where, J_w is the experimental flux, “k” is the convective mass transfer coefficient and “K” is the solute resistivity, $\pi_{D,b}$ is the bulk osmotic pressure of the draw solution, and $\pi_{F,b}$ is the bulk osmotic pressure of the feed solution. The k value can be estimated from Equation (4).

$$k = \frac{S_h D}{d_h} \quad (4)$$

In Equation (4), S_h is the Sherwood number, D is the diffusion coefficient of the draw solution and d_h represents the hydraulic diameter of the channel. The Sherwood relationship between laminar and turbulent flow can be found elsewhere (Ibrar et al., 2020b). Unfortunately, the proposed model by McCutcheon and co-workers neglect the effects of salt transport and the external mass transfer resistance on the support layer (Nagy, 2014). Yip et al. (2011) presented a modified mathematical model to predict water flux in the FO process, including the effects of internal and external concentration polarizations with reverse salt diffusion from the draw to the feed solution. Water flux in the FO process is given by Equations (5) and (6) to express the FO and the PRO operating modes, respectively:

$$J_w^{FO} = A \left[\frac{\pi_{D,b} \exp(-J_w K) - \pi_{F,b} \exp\left(\frac{J_w}{k}\right)}{1 + \frac{B}{J_w} \{ \exp(J_w/k) - \exp(-J_w K) \}} \right] \quad (5)$$

$$J_w^{PRO} = A \left[\frac{\pi_{D,b} \exp\left(-\frac{J_w}{k}\right) - \pi_{F,b} \exp(J_w K)}{1 + \frac{B}{J_w} \{ \exp(J_w K) - \exp\left(-\frac{J_w}{k}\right) \}} \right] \quad (6)$$

where B is the salt permeability coefficient, Yip’s model ignored the mass transfer resistance at the porous support layer. A general resistance in the series mathematical model was

developed by Nagy (2014), combining the effects of concentration polarization with the effect of external resistance on the porous support layer as given by Equations (7) and (8) for the FO and the PRO operating modes, respectively.

$$J_w^{FO} = A \left[\frac{\pi_{D,b} \exp\left[-J_w\left(\frac{1}{k_D} + S/D_D\right)\right] - \pi_{F,b} \exp\left(\frac{J_w}{k_F}\right)}{1 + B/J_w \left\{ \exp(J_w/k_F) - \exp\left[-J_w\left(\frac{1}{k_D} + \frac{S}{D_D}\right)\right] \right\}} \right] \quad (7)$$

$$J_w^{PRO} = A \left[\frac{\pi_{D,b} \exp\left(-\frac{J_w}{k_D}\right) - \pi_{F,b} \exp\left[J_w\left(\frac{1}{k_F} + \frac{S}{D_F}\right)\right]}{1 + B/J_w \left\{ \exp\left[J_w\left(\frac{1}{k_F} + \frac{S}{D_F}\right)\right] - \exp\left(-\frac{J_w}{k_D}\right) \right\}} \right] \quad (8)$$

In Equations 7 and 8, S is the membrane structure parameter, and D_D and D_F are the diffusion coefficient of the draw and feed solution, respectively.

Ibrar et al. (2020b) presented an alternative way to accurately measure and predict a forward osmosis process's ECP (external concentration polarization), ICP (internal concentration polarization), and water flux. The model accurately predicted the ECP and ICP in the FO process. Although the earlier models based on ideal solution and solution-diffusion theories can predict the experimental flux for the draw and feed concentration ranges used in the experiments, they do not apply to all FO applications with blended or mixed draw solutions or when specific information about FO module is not available due to propriety issues. For instance, calculating diffusion coefficient values “D” is not available for a mixture of draw solutions. Hence, it will be tedious to calculate the value of “k” and “K”. As such, where the solute resistivity “K” and mass transfer coefficient “k” values are hard to determine for a forward osmosis system, this model can provide an alternative solution. Generally, the developed FO process models account for the enteral and external CP, reverse salt diffusion, and external resistance parameters, allowing them to accurately predict water flux in the FO process.

2.1. Machine Learning models for FO process

Several researchers have developed machine learning models to successfully predict forward osmosis process performance based on experimental data (Jawad et al., 2020; K et al., 2021). In machine learning modelling, researchers collect experimental data from different publications and feed the data to a machine learning program, such as ANN (Artificial neural networks) or other algorithms such as RSM (Response surface methodology), ANFIS (Adaptive Neuro-Fuzzy Inference System), linear regression, KNN (K-nearest neighbour) and SVM (Support Vector machines). The models are trained on training data and then tested with random test data outside the training data. The model's accuracy is tested on the correlation coefficient (R^2) and the mean square error (MSE). The R^2 of the model ranges from 0 to 1, reflects how close the data is to the regression line, and can be mathematically presented by Equation (9).

$$R^2 = \frac{\sum_{k=1}^n (P_{iml} - y_{ims})^2}{\sum_{k=1}^n (y_{iactual} - y_{ims})^2} \quad (9)$$

In Equation (9), P_{iml} represents the output of the machine learning model, y_{ims} is the mean of the sample data, and $(y_{iactual})$ represents the actual output. A higher correlation coefficient generally reflects a good predictive power of a machine learning model. The R^2 value is calculated for training, validation, and testing data. If a model shows a high R^2 value for training data but presents a low R^2 value for testing data, it is prone to overfitting. The MSE is another crucial parameter to assess the predictive power of a machine learning model. The MSE is estimated by using Equation (10).

$$MSE = \frac{1}{n} \sum (y_{iactual} - P_{iml})^2 \quad (10)$$

Generally, the higher the value of R^2 and the lower the MSE, the better the predictive ability of the model.

Jawad et al. (2020) predicted forward osmosis membrane flux using ANN and obtained a high correlation coefficient (R^2) value of 97.3 for the machine-learning model. The membrane flux was predicted based on the 9 input parameters to the forward osmosis process, such as type of membrane, type of feed and draw solution and other operating conditions, details of which can be found in (Jawad et al., 2020). Ibrar et al. (2022b) predicted internal and external concentration polarisation based on input parameters in the forward osmosis process using ANN and decision tree-based algorithms. The study successfully predicted concentration polarisation based on the input parameters. K et al. (2021) used ANN, RSM and ANFIS to optimise the forward osmosis process for maximum water flux and minimum reverse salt flux. Amongst these models, ANN and ANFIS exhibited higher accuracy for optimising the process. **Figure 2** presents a hierarchy of an ANN model to predict concentration polarisation in the forward osmosis process.

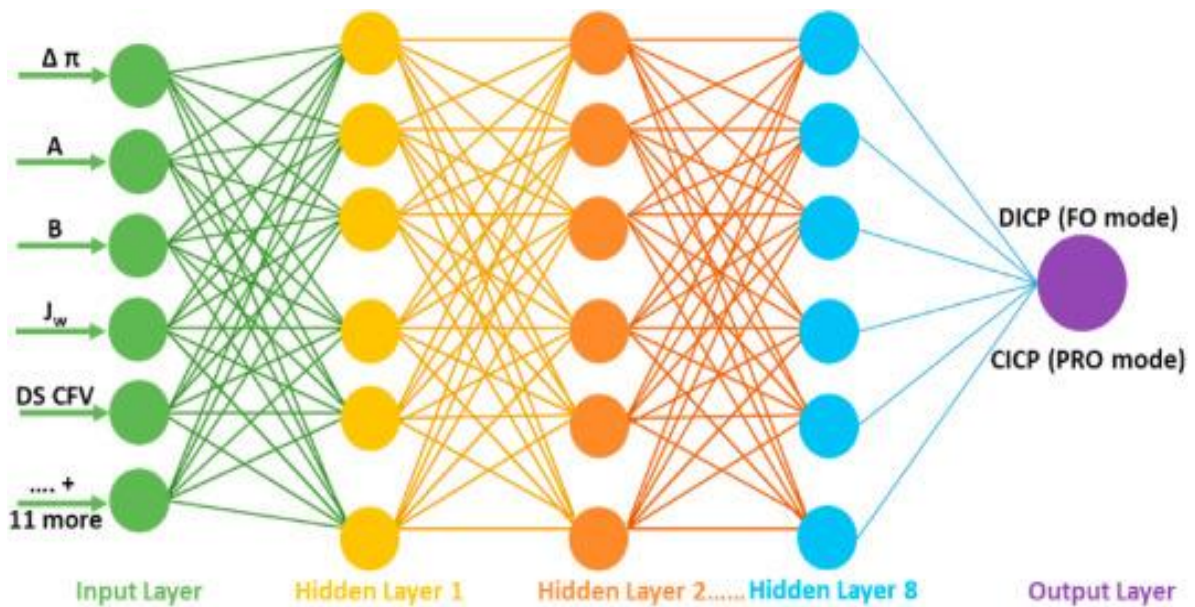


Figure 2: ANN model to predict concentration polarisation in forward osmosis. $\Delta \pi$ is the osmotic pressure gradients, A and B are the water and salt permeability coefficients, J_w is the water flux, and $DS\ CFV$ is the draw solution cross-flow velocity. The figure was adapted from (Ibrar et al., 2022b) with permission from Elsevier.

3. FO membrane

The FO membrane has been one of the most investigated parameters in the last two decades (Dsilva Winfred Rufuss et al., 2022). Different FO membranes were developed for seawater desalination to provide high water flux, low reverse salt flux (RSF), and high rejection rate. These membranes come in different configurations and materials to address certain shortcomings in the FO process or meet specific design requirements.

3.1 Commercial membranes

The most critical issues for FO membranes are the membrane design, concentration polarization (CP), reverse solute diffusion, draw solute properties, and membrane fouling (Suwaileh et al., 2018). An efficient FO membrane should have a low structure parameter (S) to reduce the effect of concentration polarization. CP is classified into two types: External concentration polarization (ECP), which appears across the membrane surface due to non-ideal hydrodynamics. ECP can be mitigated by increasing the flow velocity or turbulence or optimizing the water flux (Altaee et al., 2014). Besides, ICP occurs throughout the boundary, making it more difficult to mitigate by changing the operating conditions (Zhao et al., 2012). The membrane thickness and pore tortuosity are important variables that can affect the ICP, significantly impacting how well FO membranes work. FO membranes with large structure parameters experience severe ICP, negatively impacting water flux and membrane fouling (Altaee and Sharif, 2014). Less pore tortuosity in the support layer effectively reduced ICP for maximum water flux in the FO membranes (D. Ahmed et al., 2021). The FO membranes are commercially available for seawater desalination, although they are compatible with treating industrial and domestic wastewater, brackish waters, and other feed solutions (Lutchmiah et al., 2014). The first commercial FO membrane was introduced by Hydration Technology Innovation (HTI). The membrane was available in cellulose triacetate (CTA) and polyamide

thin-film composition (TFC) as a flat sheet or a spiral wound module. Based on the literature, the membrane specifications show a moderate water flux of 0.7 L/m²h and a relatively high salt permeability coefficient of 1.5 m/s compared to TFC and Toyobo CTA FO membranes (**Table 1**). The membrane structure parameter, 663 μm , is rather large, promoting internal concentration polarization and compromising a high permeation flux. CTA membranes are more resistant to membranes; hence, HTI CTA membranes would be suitable for wastewater treatment and impaired-aqueous feed solutions (Li et al., 2020). Compared to the HTI CTA membrane, the TFC HTI membrane has twice the structure parameter and water permeability of the HTI membrane and 5 times lower salt coefficient parameters to reduce reverse salt flux. The latter will minimize the draw solution loss in the FO osmosis and operation cost. Incorporating aquaporin technology in the FO membrane increased water flux compared to the CTA membrane introduced by the HTI Company. The Aquaporin membrane's structure parameter is 210 reduces the ICP, which would be more intensive in membranes with large structure parameters, such as HTI and Toyobo membranes. Oaysis FO membrane exhibits the highest water permeability coefficient, 3.92 Lm²h.bar, amongst all the commercial FO membranes, whilst the Porifera FO membrane exhibits a moderate structure parameter of 375 μm . Porifera Company manufactures TFC FO membranes with a high-water permeability coefficient of 2.1 Lm²h.bar and a 344 μm structure parameter to reduce ICP is introduced in flat sheet modules, making them suitable for wastewater treatment. The flat sheet modules are easy to clean compared to spiral wound (HTI & FTS) and hollow fibre (Aquaporin & Toyobo) membranes. Toyobo hollow fibre FO membranes have the largest membrane area, circa 650 m², for the HP10130 module (Ibrar et al., n.d.). The advantage of the FO module of a large membrane area is to reduce the plant's footprint, particularly commercial plants of large capacities. Although Aquaporin membranes come in hollow fibre configuration, the active membrane area is 2.3 m² for a small module and 14 m² for a large module. In practice, the

preferred FO membrane should combine the high-water flux of Oaysis and Porifera membranes and the large active membrane area of the Toyobo FO membrane. Besides, the membrane cost should be affordable as most FO membrane, apart from the HP10130 module, is several times more expensive than commercial RO membranes (Altaee et al., 2017).

Table 1: Commercial membrane specifications for the forward osmosis

Supplier	Material	A _w (LMH/bar)	B (LMH)	S (μm)	Flux (LMH)	References
HTI	CTA	0.7	1.5	663	18.6- FO mode	(Chia et al., 2020; Shadravan and Amani, 2021; Wang et al., 2015)
HTI	TFC	1.3	0.3	1227	15	(Chia et al., 2020; Ren and McCutcheon, 2014; Wang et al., 2015)
FTS	CTA	0.69	0.94	707	9.092	(Chaoui et al., 2021; Madsen et al., 2017)
FTS	TFC	1.25	0.528	471	14.906	(Chaoui et al., 2021; Madsen et al., 2017)
Aquaporin	TFC	0.43	0.139	210	13.2 FO mode 21 PRO mode	(Alihemati et al., 2020)
Oaysis	TFC	3.92	3.74	375	30	(Cath et al., 2013)
Toyobo	CTA	0.27	0.222	1024	8 -FO mode 15 -PRO mode	(Alihemati et al., 2020)
Porifera	TFC	2.1	1.2	344	33 -FO mode 58- PRO mode	(Roy et al., 2016; Suwaileh et al., 2020)

3.2 Laboratory-made membranes

High water permeability, excellent chemical stability, high mechanical strength, low concentration polarization, and low fouling propensity are all necessary characteristics of the ideal membrane for the FO water treatment process. For this reason, several research works have been carried out to fabricate high-performance CTA/CA-based FO membranes and TFN/TFC-based FO membranes. Most of these membranes were fabricated on a lab scale with different materials using the phase inversion method, interfacial polymerization (IP) technique, electrospinning, and layer-by-layer (LBL) deposition (Suwaileh et al., 2020). Phase inversion is the most significant lab-scale and effective method for creating FO membranes with a flat sheet and hollow fibre configurations. It entails dissolving a polymer in a solvent before casting

the suspension of the polymer on a support layer. The subsequent step involves precipitating this support layer by immersion, analogous to immersing a polymer solution in a non-solvent coagulant bath. Additional subcategories of this technique include thermally induced phase separation, controlled evaporation-induced precipitation, vapour phase precipitation, and non-solvent-induced phase separation (NIPS) (Suwaileh et al., 2018). However, electrospinning is a typical lab-scale method for producing collected fine fibres leading to fibrous polymers-based FO flat sheet and hollow fibre membranes using a high electrical field (Wu et al., 2021).

3.1.1. wCA/CTA-based FO membranes

As shown in **Table 2**, most studies have concentrated on using CA/CTA polymers to fabricate flat sheet and hollow fibre FO membranes by phase inversion method (PI) instead of fabricating FO nanofiber membranes by electrospinning. The ease of fabrication of CA/CTA FO membranes could explain the popularity and widespread of these FO membranes in small laboratory-scale experiments. The concentration and temperature of the casting CA/CTA polymers solution, as well as the temperature and duration of the evaporation, coagulation, and annealing processes, were among the CA/CTA membrane production factors via phase inversion method that was thoroughly investigated for their potential effects on FO membrane performance (Li et al., 2015, 2012). A spreading height of 200 μm for a solution containing 18 wt% CA, as well as the procedures of evaporating at 25 $^{\circ}\text{C}$ for 60 seconds, coagulation in a water bath at 5 $^{\circ}\text{C}$ for 24 hours, and annealing at 70 $^{\circ}\text{C}$ for an hour, were, for instance, ideal critical parameters for fabricating a CA-based FO membrane with 95.48% salt rejection performance (Li et al., 2015). However, in another work, 17.9% of CA polymer, an evaporation time of 60 seconds, a coagulation bath temperature of 12 $^{\circ}\text{C}$ and an annealing temperature of 80 $^{\circ}\text{C}$ were selected as the most suitable conditions to fabricate CA-based FO membrane with a smoother surface than commercial HTI one (Mirkhalili et al., 2017). In another study, a CTA-FO flat sheet membrane was prepared via the phase inversion technique, in which the impact

of casted membrane thickness was studied. It was found that decreasing membrane thickness could effectively enhance water flux and minimize ICP. A CTA membrane with a thickness of 50 μm achieved the highest water permeable flux of 20.3 LMH and the lowest RSF of 14.6 gMH using DI as FS and 1M NaCl as DS (G. E. Chen et al., 2017). The same high trend of water flux has been achieved for casted CTA-based FO membranes using hydrogels such as methyl-, and ethyl-, butyl-methacrylate (Ding et al., 2020). The hydrogels have increased membrane hydrophilicity and acted as the active barrier. The fabricated hydrogel-modified CTA membrane showed high pure water flux (20 LMH) and better antifouling properties. It was also noticed that using additives as non-solvents and pore-forming agents during the phase inversion method, such as lactic acid, maleic acid and methanol, could enhance casted CTA/CA-based FO membranes' water permeability and salt rejection performance to a specific limit (G. Li et al., 2013; Shang and Shi, 2018). For example, casted CTA-FO membrane salt rejection was between 95% and 98% when the lactic acid concentration was lower than 3 wt.% (G. Li et al., 2013). Moreover, forming a double dense layer during the CA polymer phase inversion technique on top of a glass plate as a casting substrate could show a less fouling propensity, higher solute selectivity and lower salt leakages (0.8 gMH) (Zhang et al., 2010). Another prototype double-skinned CA FO membrane prepared by phase inversion exhibited a water flux of 48.2 LMH using 5.0 M MgCl_2 as DS and a lower RSF of (6.5 gMH) (Wang et al., 2010).

Some studies have blended CTA and CA polymers to create the FO casting solution. CTA/CA blended-based-FO membranes showed high hydrophilicity and high-water permeability due to the hydroxyl group (-OH) presents in CA polymer (Ghosh et al., 2015; Nguyen et al., 2013). On the other hand, CA polymer was mixed with poly(vinylidene fluoride) PVDF polymer to fabricate multilayer FO membranes. CA was utilized as a hydrophilic and high porosity bottom layer to reduce the foulants accumulation (Duong et al., 2016). A

reduction of 75% of fouling propensity was observed when CA was used as a bottom layer compared to the simple FO membrane made of PVDF, woven fabric and PA (PA/PVDF) (Duong et al., 2016).

On the other hand, It was noticed that the single-casted CA membranes are insufficient for salt separation; for this reason, some studies have tried to modify the membranes through a simple coating technique using polyvinyl alcohol (PVA) with Glutaraldehyde (GA) crosslinking agent to enhance the salt rejection as well as polydopamine (PDA) coating as hydrophilicity improver (Abounahia et al., 2022; Ahn et al., 2015; Song et al., 2018). The developed CA/PVA membrane exhibited 8.8 LMH water permeable flux and 89.9% salt rejection (Ahn et al., 2015). However, CA/PVA/PDA membrane showed an osmotic water flux of 16.72 LMH and 0.14 ($\text{mol m}^{-2} \text{h}^{-1} \cdot \text{mMH}$) RSF with DI water as FS and 2.0 M NaCl as DS in the FO-mode operation. Also, it achieved a 96.4 % NaCl salt rejection (Song et al., 2018). Furthermore, creating the PA layer through IP as a thin selective layer on top of the casted CA/CTA-FO membranes has increased their salt selectivity (Han et al., 2022; Wu et al., 2018). In a Wu et al. [55] study, the prepared TFC/CTA-FO membrane by thermally induced phase separation (TIPS) method followed by crosslinking of PA active layer exhibited 11.79 LMH water flux and 96% salt rejection. While preparing TFC/CTA-FO membrane through nonsolvent-thermally induced phase separation followed by PA crosslinking has a higher water flux of 14.89 LMH and 92.63% salt rejection (Han et al., 2022). TIPS method was found to have several advantages compared to NIPS, such as easy control, a low tendency for defect formation, and diverse pore structures (Yuan Yu et al., 2017).

Another way to enhance CA/CTA-based FO membrane separation performance is by embedding pores forming additives and nanomaterials into the CTA or CA polymer casting solution (D. Ahmed et al., 2021; X. Chen et al., 2017; Li et al., 2022a; X. Wang et al., 2019). The used nanomaterials varied between Boehmite nanoparticles, titanium oxide (TiO_2), Al_2O_3 ,

zeolitic imidazolate framework-8 (ZIF-8), metal-organic framework (MOF), carbon nanotubes (CNTs), ZnO nanoparticles, graphene oxide (GO), CuO, halloysite nanotubes, UiO-66-NH₂ nanomaterial, Chitosan (CS) nanoparticles, Ti₃C₂T_x (MXene), etc. (Alfahel et al., 2020; Baniasadi et al., 2021; Chandran et al., 2022; Choi et al., 2015; Dabaghian and Rahimpour, 2015; El-Noss et al., 2020; Ghaemi and Khodakarami, 2019; Jain et al., 2021; Jamil et al., 2022; Jin et al., 2016; Kumar et al., 2018; Lakra et al., 2021; Li et al., 2016, 2022b; Lin et al., 2021; X. Wang et al., 2016; Zirehpour et al., 2015). All fabricated nanoparticles/CA-CTA FO membranes at the lab scale have shown impressive FO performance in terms of high water flux, low RSF and high salt rejection, as shown in **Table 2**. Comparable water fluxes of 58.21 LMH and 50.34 LMH have been achieved by incorporating TiO₂ nanoparticles into the CA casting solution (Jain et al., 2022, 2021). The same water flux level of 50.14 LMH and low RSF of 2.84 gMH were noticed by embedding ZIF-8 nanoparticles during membrane fabrication via phase inversion (Li et al., 2022c). Salt rejection of >97% was observed for incorporating GO into the CTA/CA blend casting solution (D. F. Ahmed et al., 2021). On the other hand, two studies have fabricated CA nanofiber-based FO membranes by the electrostatic spinning method (Shibuya et al., 2018). Water flux of 31.2 LMH, lower specific reverse salt flux of 0.03 g/L, and low structural parameter of 190 μm were all accomplished by the coaxial electrospun CA/ PVDF composite-based TFC-FO membrane (Shibuya et al., 2018). However, the dry-jet wet-spinning process created a CA hollow fibre membrane with rejection levels of 90.17% NaCl and 96.67% MgCl₂ (Su et al., 2010).

366 Table 2: Laboratory fabricated CA/CTA- based FO membranes.

Type of membrane	Material	Fabrication method	Filler	Aw (LMH/bar)	B (LMH)	S (μm)	Flux (LMH)	RSF (gMH)	Rejection %	References
Casted	CA	Phase inversion	-	NA	NA	NA	3.47 LMH	3.7 gMH	95.48% NaCl	(Li et al., 2015)
Casted	TFC/ cellulose acetate propionate	Loeb-Sourirajan wet-phase inversion method.	-	1.36 LMH/bar	0.126 LMH	680	31.8 LMH	1.6 gMH	90.4 % in RO.	(Li et al., 2012)
Casted	CA	phase inversion via immersion precipitation	-	0.584 LMH/bar	0.44 LMH	464	9.3 LMH	0.536 mol NaCl/m ² h	NA	(Mirkhalili et al., 2017)
Casted	CTA	Phase inversion	-	0.83	0.37	NA	20.3	14.6	97.35% NaCl.	(G. E. Chen et al., 2017)
Casted	CTA	Phase inversion	-	NA	NA	NA	20 LMH for BMA-CTA	19.5 gMH for BMA-CTA	NA	(Ding et al., 2020)
Casted	CA	Phase inversion	-	0.17 LMH/bar	0.07 LMH	54	10.3	0.8	51.2 % NaCl	(Zhang et al., 2010)
Casted	CA	Phase inversion	-	0.78 LMH/bar	0.46 LMH	NA	48.2 LMH	6.5 gMH	79.8% MgCl ₂	(Wang et al., 2010)
Casted	CTA	immersion precipitation-phase inversion method	Additives (lactic acid, methanol)	NA	NA	NA	10 KgMH	NA	58% NaCl	(G. Li et al., 2013)
Casted	CA	Phase inversion	PVP, maleic acid, and methanol were used as additives	NA	NA	NA	2.04 LMH	NA	95% NaCl	(Shang and Shi, 2018)
Casted	CTA/CA blend	Phase inversion	-	3.482 micron/MPa.s	0.968 microm/s	NA	NA	NA	R%=98.61% of Anthocyanin solution FRR=87.51%	(Ghosh et al., 2015)
Casting	CTA/CA	phase inversion via immersion precipitation	-	NA	NA	NA	10.39 LMH	0.084 mol NaCl/m ² h	84%	(Nguyen et al., 2013)
Casted	CA/PVA/PDA	non-solvent-induced phase separation	-	NA	NA	NA	16.27 LMH	0.14 mMH	99.533% NaCl	(Song et al., 2018)
Casted	PVA/CA	Phase inversion	-	NA	NA	NA	8.8 LMH	NA	96.4% NaCl	(Ahn et al., 2015)
Casted	PA/PVDF/CA	non-solvent-induced phase separation	-	1.1 LMH/bar	0.37 LMH	380	53 LMH	6 gMH	89.9% NaCl	(Duong et al., 2016)
Casted	CTA	thermally induced phase separation (TIPS)	-	NA	NA	NA	9.49 LMH	4.86 gMH	91.1%	(Yuan Yu et al., 2017)
Casted	TFC/CTA	nonsolvent-thermally induced phase separation (N-TIPS) process.	-	0.90 LMH/bar	0.35 LMH	384.8	14.89 LMH	4.67 gMH	NA	(Han et al., 2022)
Casted	TFC/CTA	thermally induced phase separation (TIPS) method	-	1.52 LMH/bar	0.27 LMH	516	11.79 LMH	7 gMH	92.63 %	(Wu et al., 2018)
Casted	CTA/CA	phase inversion via immersion precipitation method	Boehmite nanoparticles	1.43 LMH	5.1×10 ⁻⁸ m/s	NA	22 LMH	6 gMH	96%	(Zirehpour et al., 2015)
Casted	CA	phase inversion method	ZIF-8	NA	NA	NA	50.14 LMH	2.84 gMH	NA	(Li et al., 2022c)
Casted	CA	phase inversion method	MWCNTs	NA	NA	NA	14.11	1molMH	NA	(Choi et al., 2015)
Casted	CTA	phase inversion method	Carboxylated carbon nanofibres (CNFs)	2.1 LMH/bar	26.1×10 ⁻⁸ m/s	600 μm	15.6	1 gMH	87% NaCl	(Dabaghian and Rahimpour, 2015)
Casted	CA	phase inversion	TiO ₂	NA	NA	NA	58.21 LMH	16.28 gMH	75.9% NaCl	(Jain et al., 2022)

Type of membrane	Material	Fabrication method	Filler	Aw (LMH/bar)	B (LMH)	S (μm)	Flux (LMH)	RSF (gMH)	Rejection %	References
Casted	CA	phase inversion	TiO ₂	NA	NA	NA	50.34 LMH	13.33 gMH	NA	(Jain et al., 2021)
Casted	CA	Phase inversion	Aluminium fumarate (AlFu) metal-organic framework (MOF)	NA	NA	NA	17 LMH	2.89 gMH	85% MgCl ₂ FR >80%	(Lakra et al., 2021)
Casted	CA	Phase inversion	TiO ₂ and Al ₂ O ₃	2.40 LMH/bar	11.27×10 ⁻⁸ m/s	450 μm	15 LMH	5.4 gMH	86.8 % NaCl	(Baniasadi et al., 2021)
Casted	CTA	non-solvent-induced phase inversion	Pore-forming additives LA/ZnCl ₂	1.83 LMH/bar	0.13LMH	NA	11.5 LMH	NA	98.3% NaCl	(X. Chen et al., 2017)
Casted	CTA/CA	Phase inversion	Maleic acid as a pore-forming additive. Al ₂ O ₃	1.8 LMH/bar	4.7×10 ⁻⁷ m/s	870	27.1	10.3	81% salt rejection.	(D. Ahmed et al., 2021)
Casted	CA	phase separation technique	Dopamine-modified halloysite nanotubes (DHNT)	2.7 LMH/bar	22×10 ⁻⁸ m/s	NA	16 LMH	1.1 gMH	NA	(Kumar et al., 2018)
Casted	CA	Phase inversion	Ti3C2Tx (MXene)	NA	NA	NA	12.2 LMH	110 gMH	-	(Alfahel et al., 2020)
Casted	CTA/CA	phase inversion technique.	GO nanosheets	NA	NA	NA	33.6 LMH	1.5 gMH	>97%	(D. F. Ahmed et al., 2021)
Casted	CA	phase inversion technique.	GO	NA	NA	NA	18.43 LMH	4.1 gMH	NA	(X. Wang et al., 2016)
Casted	TFC/CTA	phase inversion method	GO Prepared from Palm Fronds	17.41 LMH/bar	2.765 LMH	NA	35 LMH	1.8 gMH	86%	(Jamil et al., 2022)
Casted	TFN/CA	Phase inversion	GO+0.81CuO	NA	NA	NA	48 LMH	0.81 gMH	NA	(Chandran et al., 2022)
Casted	CTA	Phase inversion	GO	3.67 LMH/bar	182.72×10 ⁻⁸ m/s	670	NA	NA	53.23%	(Li et al., 2016)
Casted	CA	phase inversion method	ZnO nanoparticles	NA	NA	NA	26.57 LMH	NA	99.5%	(El-Noss et al., 2020).
Casted	CA	phase-inversion method.	MIL-53(Fe)@γ-Al ₂ O ₃	NA	NA	NA	37.1 LMH	1.78 gMH	NA	(Li et al., 2022a)
Casted	CA	phase inversion method	Chitosan (CS) nanoparticles	3.8 LMH/bar	0.91 LMH	130	31.2 LMH	0.09 gMH	89.7% NaCl	(Ghaemi and Khodakarami, 2019)
Casted	CA	phase inversion via immersion precipitation	MWCNTs	NA	NA	NA	27.1 LMH	0.2807 mol NaCl/m2h	NA	(Jin et al., 2016)
Casted	CA	phase inversion	MIL-53(Fe)	NA	NA	NA	34.9 LMH	2.02 gMH	NA	(X. Wang et al., 2019)
Casted	CTA/CA	Phase inversion	covalent organic frameworks (COFs)	1.35 LMH/bar	0.16 LMH	520	13.34 LMH	2.13 gMH	96.3%	(Lin et al., 2021)
Casted	CA	Phase inversion	UiO-66-NH ₂ nanomaterial	NA	NA	NA	52.32 LMH	2.43 gMH	NA	(Li et al., 2022b)
Nanofibre	CA hollow fibre	Dry-jet wet-spinning process	-	0.47 LMH/bar	NA	NA	7.3 LMH	0.53 gMH	90.17 % NaCl 96.67 % MgCl ₂	(Su et al., 2010)
Nnaofibre	TFC/PVDF+CA	Electrospinning	-	2.79 LMH/bar	0.07 LMH	190	31.2	0.03	NA	(Shibuya et al., 2018)

3.1.2. TFC/TFN-based FO membranes.

Recently, TFC membranes have attracted more attention in FO applications due to their effective separation performance in water flux and efficient solute rejection (Xu et al., 2022). The TFC membranes typically have two layers: a support layer that provides the necessary mechanical backing and a thin selective layer that allows water molecules to pass through while blocking salts and other contaminants. The interfacial polymerization (IP) reaction between *m*-phenylenediamine (MPD) aqueous solution and 1,3,5-benzenetricarbonyl trichloride, also known as trimesoyl chloride (TMC) organic solution on the support layer is usually used to create the selective thin layer or the polyamide (PA) rejection layer. Different TFC porous support layers have been fabricated based on various polymers using phase inversion and electrospinning techniques. For example, a TFC membrane made of a porous polysulfone (PSf) substrate via phase inversion has achieved high FO water flux and better selectivity due to the fabricated porous substrate with finger-like pore structures and the created thin dense PA layer via conventional IP reaction (Phillip et al., 2010; Wei et al., 2011). Because the substrate significantly influences the creation of the PA layer, it is crucial to optimize and alter the membrane substrates to increase FO performance and reduce the ICP phenomenon. Thus, a hydrophilic polymer such as sulphonated polysulfone (SPSF) has been blended with a polysulfone casting solution to enhance membrane morphology and hydrophilicity (Han et al., 2012). In another experimental work, SPSF was blended with a polyethersulfone (PES) matrix to modify the substrate's hydrophilicity and maintain the membrane's long-term stability (Qiao et al., 2012). Moreover, other studies have fabricated nanofiber-based thin film composite (NTFC) membranes made of an electrospun nanofibrous substrate to provide minimal tortuosity and thickness coupled with high porosity substrate layer instead of phase inversion-based substrates (Shokrollahzadeh and Tajik, 2018). Nanofiber membranes often had high osmotic flow and low structural parameter values, making this a good method for

manufacturing FO membranes (Pan et al., 2017). According to Bui et al. (2011), commercial (HTI-CTA) FO membranes were outperformed by NTFC membranes produced from blended PSf and PES nanofibrous substrates in terms of water flux by a factor of two to five. Additionally, in contrast to conventional HTI-FO membrane with 6.5 LMH flux and 92% rejection of the same thickness, a new electrospun nanocomposite FO membrane with a scaffold-like nanofiber support layer and a 50 μm thickness was developed by Song et al. (2011). This membrane achieved a salt rejection of 97% and 37.8 LMH water permeable flux.

Several research studies looked into the introduction of inorganic nanomaterials into the substrate polymer matrix to achieve a suitable blended substrate structure with high porosity, hydrophilicity, and low tortuosity, as well as to increase membrane antibacterial activity and thermal stability like graphene oxide (GO) (Park et al., 2015), titanium dioxide (TiO_2) (Emadzadeh et al., 2014), layered double hydroxide nanoparticles (Lu et al., 2016), charcoal-based carbon nanomaterial (Hadadpour et al., 2021), and carbon nanofibers (Tavakol et al., 2020). Another way for adding these hydrophilic nanomaterials is to add them to the active layer of the TFC membrane to fabricate a thin film nanocomposite membrane (TFN) with high water permeability and low reverse solute flux (Amini et al., 2013; Shokrgozar Eslah et al., 2018). For instance, adding graphene quantum dots (GQDs) into the aqueous phase of the PA layer has increased the rejection performance of fabricated PVDF membrane resulting in 98% of salt rejection due to the formed negative surface charge (Maiti et al., 2020). The high-water permeability of 2.457 LMH/bar was achieved due to the water channels formed between the GQDs nanoparticles and the IP active layer (Xu et al., 2019). It is noticeable from **Table 3** that the fabricated TFC-based FO membranes showed a better performance with lower structural parameters and promised results compared to the commercially available TFC-FO membranes from HTI. Generally, TFC and NTFC FO membranes could be manufactured with a smaller structure parameter than the CTA, enabling them to minimize the ICP and achieving better

418 water flux. Also, the rejection of laboratory made TFC and NTFC membrane is higher than the
419 CA and CTA membrane, justifying their higher performance and economic benefits.

Table 3: Laboratory fabricated TFC/TFN-based FO membranes.

Type of membrane	Material	Fabrication method	Filler	A_w (LMH/bar)	B (LMH)	S (μm)	Flux (LMH)	RSF (gMH)	Rejection (%)	References
TFC	PSf	Phase inversion (TiO_2) IP	TiO_2	1.96 LMH/bar	10.66×10^{-8} m/s	420	17.1	2.9 gMH	92.7%	(Emadzadeh et al., 2014)
TFC	PES-SPSF	Loeb-Sourirajan wet-phase inversion method	-	0.77 LMH/bar	0.11 LMH	238	26 LMH	8.3 gMH	93.5% NaCl 96.6% MgCl_2 97.8% MgSO_4	(Qiao et al., 2012)
TFC	PSf	Phase inversion IP (GO)	GO	6.52×10^{-12} m/s.Pa	18.7×10^{-8} m/s	-	14.5 LMH	2.6 gMH	88%	(Shokrgozar Eslah et al., 2018)
TFN	PSf	Phase inversion (PSF/GO) IP	GO	1.76 LMH/bar	0.19 LMH	191	19.77 LMH	3.44 gMH	98.71 % by RO	(Park et al., 2015)
TFC	PSf	Phase inversion IP	-	1.16 LMH/atm	-	492	18 LMH	-	97%	(Phillip et al., 2010)
TFN	PVDF	Crystallization-induced phase separation IP (GQDs)	GQDs	-	-	-	170 LMH by RO.	-	Monovalent salt R= 94%. Divalent salt R = 98% Dyes (85%-90%).	(Maiti et al., 2020)
TFN	Commercial PAN	IP (GQDs)	GQDs	2.547	0.19	-	12.9	1.41 gMH	96.8 by RO	(Xu et al., 2019)
TFN	Polyethersulfone (PES)	Phase inversion (CNM) IP	Charcoal-based carbon nanomaterial (CNM)	1.79	0.19	883.4	12.08 LMH	2.97 gMH	91.33%	(Hadadpour et al., 2021)
TFN	PSf	Phase inversion (CNFs) IP	Carbon nanofibres (CNFs)	1.84 LMH/bar	0.12	788.2 μm	13.08 LMH	3.14 gMH	94.5% by RO	(Tavakol et al., 2020)
TFN	PSf	Phase inversion IP (MWCNTs)	Multi-walled carbon nanotubes	3.6 LMH/bar	2.86×10^{-8} m/s	380 μm	39 LMH	2.4 gMH	89.3 by RO	(Amini et al., 2013)
TFC	sulphonated poly(ether ketone) (SPEK) into polysulfone (PSU)	Phase inversion IP	-	0.75	0.068	107	35 LMH	7 gMH	89.5%	(Han et al., 2012)
TFC	PSf	Phase inversion. IP	-	1.78 LMH/bar	9.4×10^{-8} m/s	670	12 LMH	4.9 gMH	93.4%	(Wei et al., 2011)
TFN	PSf	Phase inversion (LDH-NPs) IP	Layered double hydroxide nanoparticles (LDH-NPs)	0.61 LMH/bar	0.27 LMH	148	18.1 LMH	8.1 gMH	-	(Lu et al., 2016)
TFC	Cyanoethyl cellulose (CEC)+ PVP Cellulose carbamate (CC)	Phase inversion. IP	-	1.17 LMH/bar	0.20	922	9.10 LMH-FO 20.67 LMH-PRO	1.35 gMH-FO 2.24 gMH-PRO	-	(Zheng and Zhou, 2019)
TFC	polyvinyl chloride (PVC)	Phase inversion IP	-	1.86 LMH/bar	9.25×10^{-8} m/s	337	22 LMH-FO 40.40 LMH-PRO	2.25 gMH-FO 4 gMH-PRO	95.13%	(Zheng et al., 2021)
TFC	PSF/PAN	Electrospinning IP	-	3.68 LMH/bar	0.32 LMH	34	38.3 LMH	10.1gMH	97.12 % NaCl	(Shokrollahzadeh and Tajik, 2018)
N-TFC	PSF/PES	Electrospinning IP	-	2.68×10^{-9} m/KPa s	3.08×10^{-10} m/s	-	33.6 LMH	4.62×10^{-2} gMH	-	(Bui et al., 2011)
N-TFC	PES	Electrospinning IP	-	1.70	-	80	37	-	97%	(Song et al., 2011)
N-TFC	PAN	Electrospinning IP	-	1.47 LMH/bar	0.278 LMH	168	41 LMH	8.61 gMH	99.8% TC wastewater.	(Pan et al., 2017)

3.3- Drawbacks

The backbone of a successful FO process is a membrane. Previous studies have shown that asymmetric membranes perform poorly in FO processes. ICP, salt precipitation, and mass transport resistance within the porous structure are all impacted by the support layer's porosity. The permeability of the thin film created on top may also be impacted by the variation in the support layer's pore structure (Ramon et al., 2012; Ramon and Hoek, 2013). It was proposed that the morphology of the selective layer can be modified by the chemistry and pore structure of the support layer, suggesting a strong relationship between the surface morphology, the support layer structure, and the functionality of the rejection layer. It is widely acknowledged that surface porosity may cause variations in the structural parameters of the FO membrane. Numerous research looked into the possibility that the micro-porous support layer could prevent mass transfer, resulting in severe internal concentration polarization (ICP) (Manickam and McCutcheon, 2017; Shaffer et al., 2015).

The DS characteristics are yet another crucial element since ICP might induce RSF and poor water flux if the DS concentration was lowered within the dense support layer. The RSF, which seems inevitable in the FO process, especially for small draw solutes, due to the concentration gradient between the FS and DS, is one of the other technical challenges. Reverse solute flux can cause membrane fouling and a significant reduction in water flux, especially when using colloidal particles and organic macromolecule draw solutions (Hoover et al., 2013). There is little documented research on preventing the fouling of FO membranes. Additionally, the FS and DS traits are among the most important considerations. For instance, to avoid ICP effects that negatively impact membrane performance, the concentration and viscosity of the DS should be controlled. Enhancing the membrane's selectivity is also crucial for preventing the impact of salt back-diffusion. Realizing FO as a workable desalination technique without a suitable membrane is challenging. The support layer should be very porous, thin, and water-

permeable to increase the membrane permeability. Low ICP, high permeance, antifouling, chemical stability, sustained mechanical strength stability, and minimum RSF is desirable properties of the ideal FO membrane (Chung et al., 2012; Wei et al., 2011). Due to these limitations, research is required to alter the FO membrane's structural characteristics and enhance its final performance to meet real-world implementation standards.

Despite the impressive performance of laboratory-made FO membranes, additional testing is required to validate their long-term performance, fouling propensity and selectivity. Before commercialisation, the polymer's chemical stability and mechanical strength should be validated in the field environment. The fabrication cost and pilot plant test of the FO membrane are essential steps before membrane commercialization. However, these steps are out of the scope of many laboratory-based studies due to time or budget limitations. Therefore, pilot plant tests and cost analyses should be included in laboratory studies, knowing the difficulties of estimating the cost of chemicals provided in small quantities from designated suppliers compared to wholesale chemicals.

4. FO membrane fouling

Although FO has been recognized as a low-fouling technology, membrane fouling is one of the main problems influencing the FO membrane performance. Membrane fouling is responsible for the water flux decline due to the membrane's pores blocking and forming a cake layer on the membrane surface. Common fouling materials are inorganic chemicals, colloidal or particulate debris, dissolved organics, chemical reactants, microbes, and microbial products (Ibrar et al., 2019). Fouling can also introduce additional hydraulic resistance and has unfavourable effects that may lead to membrane deterioration. Researchers applied several technologies to maintain the membrane's water flux and mitigate membrane fouling, including using antifouling FO membranes, feed and draw (if applicable) solutions pretreatment,

optimizing the operation parameters, and membrane physical and chemical cleaning. Besides, it is worth mentioning that the fouling in the FO membrane can be divided into external and internal fouling, depending on the utilized membrane orientation. Pore blockage or internal fouling caused by smaller foulants is the most serious and extremely difficult to remove (Ibrar et al., 2019). Nevertheless, by altering the feed water's properties or using chemical cleaning, external or surface fouling can be easily regulated compared to internal fouling.

Several experimental works have employed low-fouling membrane materials to enhance different FO-based membranes' antifouling performance, as shown in **Table 4**. For example, Y. Wang et al. (2018) have fabricated new TFC-FO membranes with excellent antifouling performance against seawater as a model foulant using dopamine (DA) as an antifouling material in the aqueous phase during the IP technique. As well as the enhanced membrane surface hydrophilicity and smoothness have contributed to enhancing the FO membrane antifouling performance in which fewer foulants attachment occurs on the membrane surface (Wang et al., 2018). In another study, functionalized multi walls carbon nanotubes (MWCNT)-cellulose acetate (CA)-based membrane showed a 57% decrease in water flux after the alginate fouling test in the FO process compared to a bare CA membrane (Choi et al., 2015). The acid-treated MWCNTs increased the membrane's surface negative charge, leading to a potent aversion to alginate foulant. However, functionalizing CNTs with polydopamine (PDA) has exhibited superior antifouling properties (Deng et al., 2020; Song et al., 2015). For instance, incorporating CNTs in PDA as an aqueous phase for the PA layer formation on top of PSf substrate successfully showed considerable good antifouling membrane performance in the FO process by achieving 81.4% water flux recovery after a third cycle of humic acid fouling test and cleaning (Song et al., 2015). While using MXENE to improve membrane fouling resistance decreased the water flux of the CA membrane by only 10.7% after using treated sewage effluent (TSE) feed solution compared to distilled water (DW) feed solution (Alfahel et al., 2020).

Organic metal frameworks (Lakra et al., 2021), zwitterion (Chiao et al., 2019), layered double hydroxides (LDH) nanosheets (Bagherzadeh et al., 2023), graphene quantum dots (GQDs) (Seyedpour et al., 2018), graphene oxide (GO), chitosan (CS) (Salehi et al., 2017) and other materials also employed in the literature to enhance the FO membrane fouling resistance (L. Wang et al., 2019).

Other than employing low-fouling membrane materials, several researchers have used various strategies in the FO process to mitigate FO membrane fouling, as shown in **Figure 3**, such as implementing different cleaning techniques and optimizing the system's operational conditions (Ibrar et al., 2020c; Im et al., 2021; Lee et al., 2020; Liu et al., 2020; Yadav et al., 2020b; Youngbeom Yu et al., 2017). Cleaning strategies include chemical treatment (Ab Hamid et al., 2018; Ibrar et al., 2022a, 2021), biological cleaning (Yadav et al., 2020b), physical cleaning, e.g. DI water bubbling, osmotic backflush (Ibrar et al., 2021, 2020c), air scouring, increasing feeds cross-flow velocity (Youngbeom Yu et al., 2017) and altering membrane orientation (Ibrar et al., 2021). The chemical cleaning methods use alkaline/acid solutions, surfactants, or chelating agents to remove organic, inorganic and colloidal particles (Ab Hamid et al., 2018; Ibrar et al., 2020a; Liu et al., 2020; Youngbeom Yu et al., 2017). These methods were proven effective in treating a wide range of organic and inorganic fouling, especially when the feed or draw solution is of low quality, e.g. wastewater (Ibrar et al., 2020a; Khanafer et al., 2021a). Despite the effectiveness of chemical cleaning, it has some drawbacks, such as the cost of chemicals and secondary wastewater generation. Alternatively, physical methods were proposed for the FO membrane cleaning and fouling mitigation. Physical cleaning methods were effective for organic and inorganic fouling mitigation, including altering the cross-flow velocity, cleaning with hot water, air-scouring, and osmotic backwashing (Youngbeom Yu et al., 2017). Nevertheless, many variables affect cleaning effectiveness and should be considered during the proper selection of the cleaning technique, such as the

temperature, pH, the sequence of the cleaning steps and the compatibility of the FO membrane material (Lee et al., 2020; Yadav et al., 2020b). Compared to chemical cleaning, Ibrar and co-workers (2020c) demonstrated that FO membrane cleaning with hot water at 35 °C after landfill leachate treatment could recover 97% of the water flux in multiple filtration cycles. Osmotic backwash cleaning was slightly less effective than cleaning with hot water and achieved 95% to 91% water flux recovery in filtration cycles one to four. The effectiveness of physical cleaning methods is on par with the chemical ones but with merits for being less aggressive on the membrane, as will be discussed below.

In addition to the cleaning methods mentioned above, membrane fouling could be controlled by optimizing the operating conditions, e.g. changing the membrane orientation (AL-DS vs AL-FS), using spacers, FO recovery rate, and pretreatment of feed/draw solution. The fouling mechanism is more intricate in the PRO mode (when the active layer faces the DS) (Ibrar et al., 2020a; Khanafer et al., 2021a). In contrast, the filtration process is more stable and cleaning effectiveness is better in FO mode (when the active membrane area faces the FS), which would decrease water flux (Ibrar et al., 2021, 2020a; Khanafer et al., 2021b). For example, FO membrane osmotic backwashing after wastewater treatment restored 95% to 91% of the declined water flux when the FO operated in the AL-FS and 90% to 68% when it operated in the AL-DS coordination (Liu et al., 2020). In another experiment, using spacers in the FO process treating a dewatered construction wastewater resulted in almost half the water flux achieved in the FO process without a spacer, showing that spacers used in the FO membrane could negatively impact the process performance (Chia et al., 2020). Additionally, construction wastewater prefiltration with a multimedia sand filter resulted in a 35% increase in the water flux compared to the FO experiment without feed prefiltration (Shadravan and Amani, 2021).

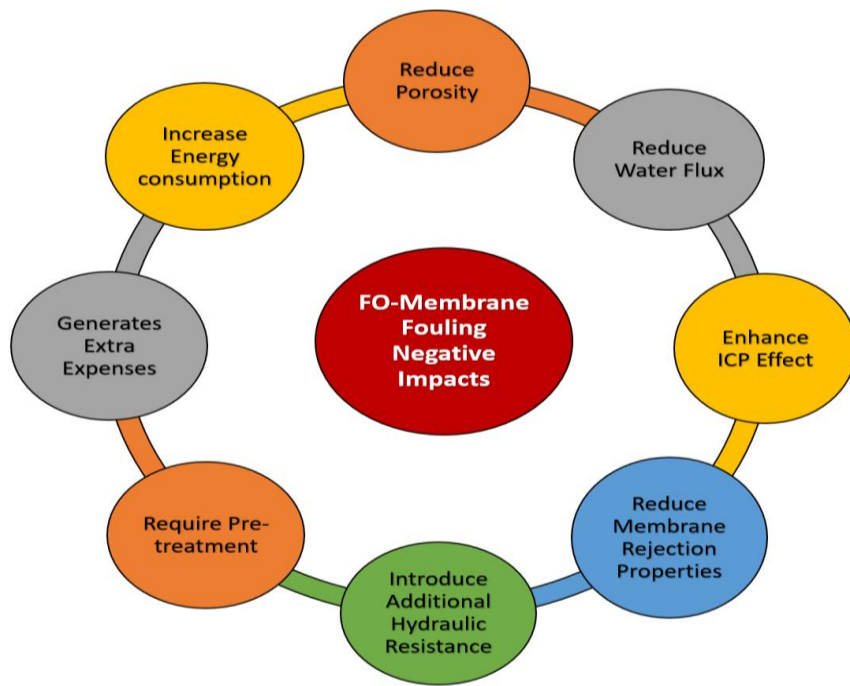


Figure 3: Negative impacts of FO-membrane fouling.

546 Table 4: FO membranes and antifouling performance.

Membrane Type	Model Fouling tests	Orientation	Cleaning and control strategy	Antifouling performance results	References
Functionalized MWCNTs blended CA membranes	FS foulant: Alginate DS: 3M NaCl	FO-mode	Not conducted.	Reduction of Water flux decline (%) = 57%	(Choi et al., 2015)
(CS)-AlFu MOF-CA membrane	FS foulant: Synthetic wastewater (SW) and real wastewater (RW) DS: 1M MgCl ₂	FO mode	DI backwashing and flushing with tap water	Over 80% of water recovery	(Lakra et al., 2021)
MXene-CA membranes	FS foulant: Treated sewage effluent (TSE) DS: Seawater	FO mode	Not conducted.	Water flux decreased by 10.7%	(Alfahel et al., 2020)
TFC- brush-grafted PSf membrane	FS foulant: 500 ppm BSA DS: 2M NaCl	FO mode	DI physical cleaning	FRR%= 95% after 8 cycles Water flux decline (%) = 10%	(L. Wang et al., 2019)
TFC (dopamine)-PSf support layer	FS foulant: Seawater DS: 0.5-4M NaCl	FO mode	DI physical cleaning	Water flux decline = 14.4%	(Wang et al., 2018)
TFN (LDH)-PES membrane	FS foulant: Sodium alginate (SA) added to the synthetic wastewater DS: 1M NaCl	FO mode	Not conducted	Water flux reduction = 22.88%	(Bagherzadeh et al., 2023)
TFC-polydopamine/ CNTs- PSF membrane	FS foulant: Humic acid (HA) DS: 2M MgCl ₂	PRO mode	DI backwashing	Water flux recovery= 81.4% after 3 cycles	(Song et al., 2015)
PDA-SWCNTS-PES MF membrane	FS foulant: BSA DS: 1M NaCl	PRO-mode	Not conducted	Flux declined by 19%	(Deng et al., 2020)
TFC (GQDs)-PES membrane	FS foulant: Alginate and E. coli. DS: 1M NaCl	FO mode	Physical cleaning	Water flux recovery = 35%	(Seyedpour et al., 2018)
CS/GO bilayers on the SPES/PES substrate.	FS foulant: SA DS: 1M Na ₂ SO ₄	FO mode	Physical cleaning	Water flux recovery = 78%	(Salehi et al., 2017)
TFC FO membrane from Porifera	FS foulant: TSE DS: Brine MSF	PRO mode	DI water cleaning at 40 °C and 2 LPM flow rate.	Water flux decline (%) = 22% at the end of cycle 4.	(Khanafer et al., 2021a)
CTA membrane from HTI	FS foulant: Wastewater DS: 35 g/L NaCl	FO mode	Chemical cleaning (free nitrous acid)	Free nitrous acid recovered 74% of water flux.	(Ab Hamid et al., 2018)
TFC (PA+ PSf support layer)	FS foulant: Landfill leachate wastewater DS: 0.6 M NaCl	FO mode PRO mode	Chemical cleaning (hydrogen peroxide (H ₂ O ₂)) Osmotic backwashing	Water flux recovery = 98% in FO mode Water flux recovery= 90% in PRO mode	(Ibrar et al., 2021)
CTA membrane from HTI	FS foulant: Activated sludge DS: 3M NaCl	NA	Physical cleaning (increasing cross-flow velocity and air scouring)	By Osmotic backwashing Water flux recovery = 99.9% after 1 min.	(Youngbeom Yu et al., 2017)
Zwitterionic TFC TFC(AEPPS)-PSf substrate	FS foulant: SA DS: 2M NaCl	FO mode	Not conducted	Normalized water flux =76% after 800 min	(Chiao et al., 2019)
TFC FO membrane from Porifera	FS foulant: Seawater of a 45 g/L at 25 °C DS: Seawater of 80 g/L at 40 °C	FO mode	DI water cleaning	Flux recovery of 93%	(Khanafer et al., 2021b)
TFC FO membrane from Porifera	FS foulant: Wastewater DS: Synthetic seawater (35 g/L NaCl)	FO mode	Physical and chemical cleaning	Water flux recovery rate =110% by chemical cleaning	(Im et al., 2021)
CTA membrane from Sterlitech	FS foulant: Landfill leachate wastewater DS: 1M NaCl	FO mode PRO mode	Chemical cleaning (Sodium docusate)	Water Flux recovery= 99%	(Ibrar et al., 2022a)
CTA from FTS	FS foulant: Landfill leachate wastewater DS: 0.6 M NaCl	FO mode PRO mode	Physical cleaning (hot water at 35 °C and osmotic backwashing) Chemical cleaning by H ₂ O ₂	Water Flux recovery= 100% by H ₂ O ₂ .	(Ibrar et al., 2020c)

4.1. Practical implications:

Membrane fouling is still a significant operational issue, and therefore, developing solutions for fouling mitigation and a thorough understanding of membrane fouling behaviour is imperative. New antifouling membranes exhibited good resistance to organic and inorganic fouling, but they have some drawbacks, such as the cost of the membrane and long-term performance. For example, graphene oxide (GO) and CNT were tested in the laboratory but are expensive to fabricate and commercialize (Ibrar et al., 2020a). In addition to the high fabrication costs, these membranes' long-term and pilot plant performance is not confirmed since most published research was laboratory-based.

Chemical cleaning methods are effective and widely used for reverse osmosis desalination plants but have several drawbacks worth considering. Most notably, chemical cleaning generates a secondary waste solution that requires additional management. Also, chemical cleaning compromises the selective membrane layer integrity, affecting the membrane water flux and rejection rate (Ibrar et al., 2022c). For example, most FO membranes are sensitive to oxidants, such as chlorine, that would damage the selective membrane layer. Cellulose triacetate membranes, in contrast, are sensitive to high and low pHs used in cleaning (Lee et al., 1981).

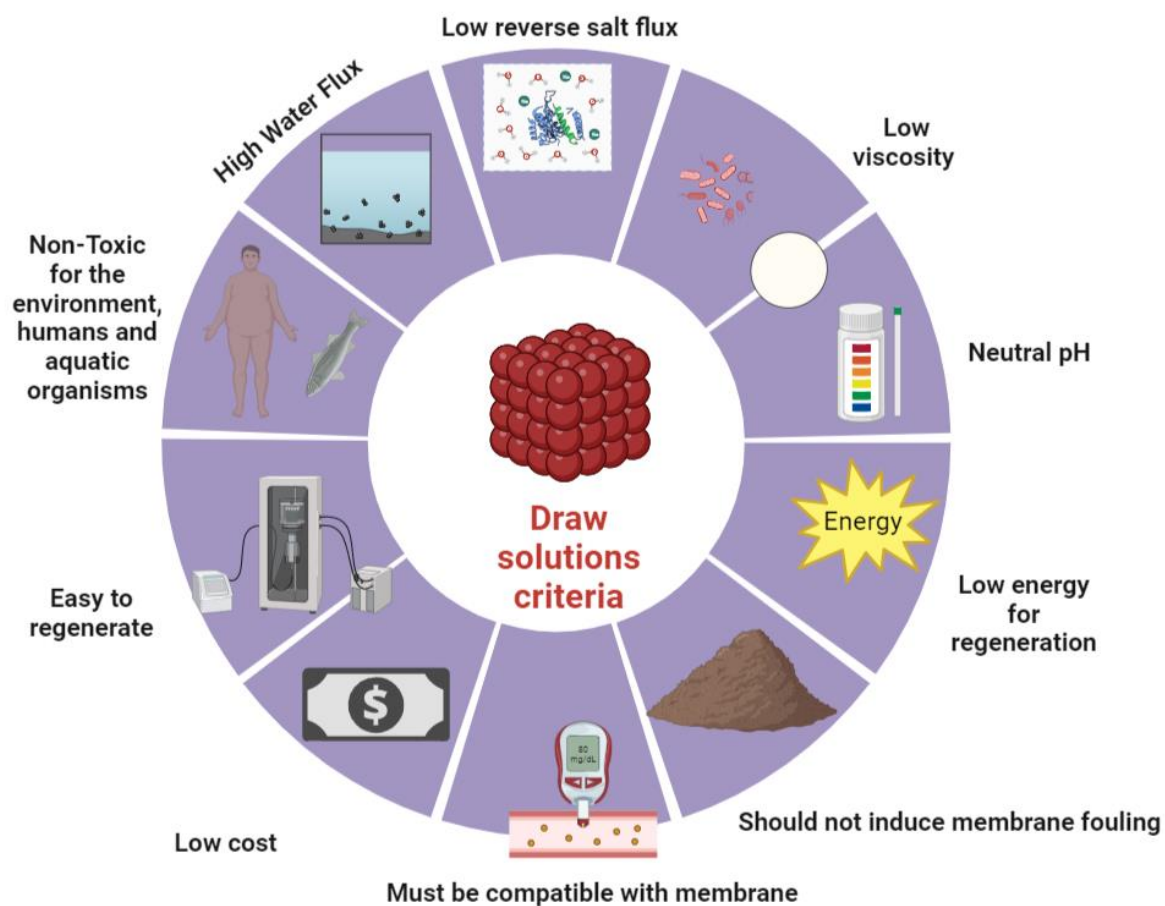
Physical cleaning methods have more potential for fouling mitigation in the FO process (Khanafer et al., 2021b; Liu et al., 2020). Membrane cleaning with hot water, 35 °C to 40 °C, is an effective method for removing organic and inorganic fouling without affecting the membrane integrity, as in chemical cleaning (Khanafer et al., 2021b; Liu et al., 2020). Most FO membranes tolerate up to 40 °C feed temperature, knowing that the cleaning process lasts for 30 min to 60 min only. A waste-heat source from industrial processes could heat the cleaning solution. Likewise, osmotic backwash cleaning showed good results in recovering

water flux in fouled membranes, although it is less efficient than hot water cleaning (Liu et al., 2020). The RO brine could be the draw solution used in backwash cleaning to reduce the cost of chemicals while avoiding wastewater generation (Khanafer et al., 2021b). Another physical cleaning method is increasing the cross-flow velocity (CFV) of the feed/draw solution to reduce the concentration polarization effects (Chun et al., 2017). Therefore, increasing the CFV has a limited impact on the fouling mitigation compared to the backwash and hot water cleaning methods. Generally, physical cleaning with hot water and osmotic backwash could replace the chemical cleaning methods of FO membranes. The advantages of physical cleaning include a cost-effective method, suitable for organic and inorganic fouling, no impact on the selective membrane layer, and eliminating chemical wastewater generation as in the chemical cleaning methods (Ibrar et al., 2021; Liu et al., 2020).

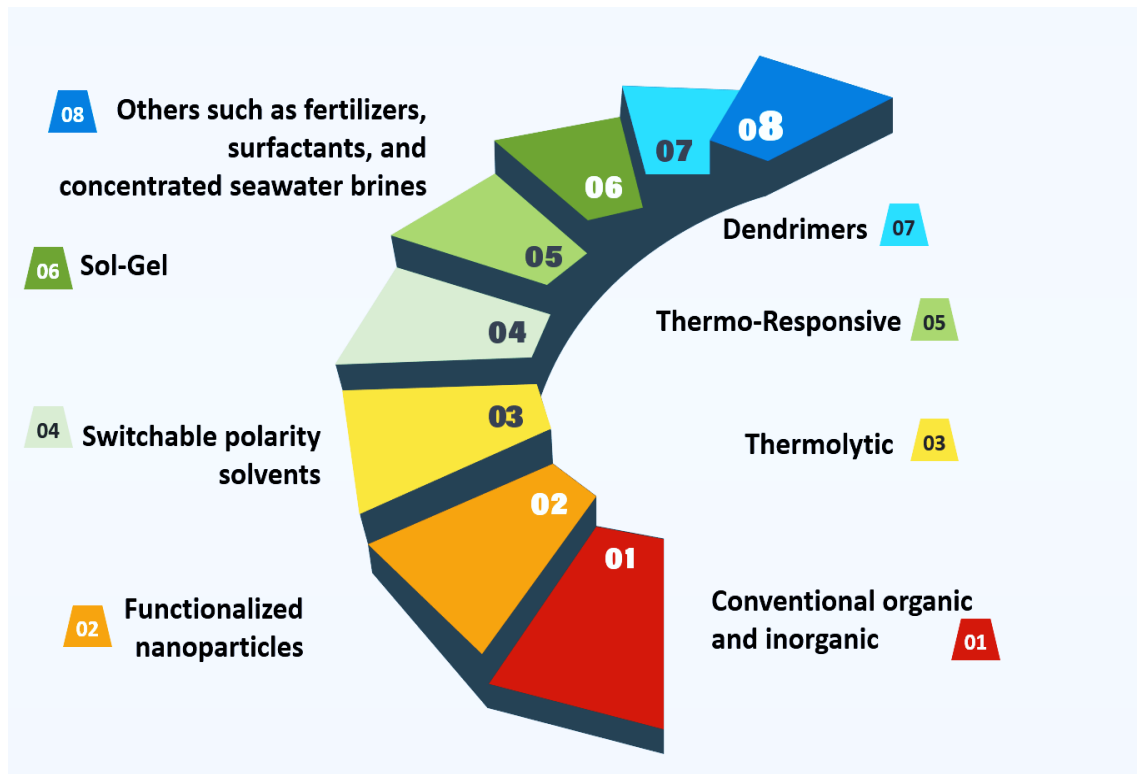
Changing the membrane orientation is another method for reducing the FO membrane fouling by manipulating the operating conditions (Ab Hamid et al., 2018; Ibrar et al., 2020a). Nevertheless, changing membrane orientation will alleviate membrane fouling but not eliminate it, and it is often combined with physical or chemical cleaning methods for water flux recovery (Ab Hamid et al., 2018; Youngbeom Yu et al., 2017). The polluted solution is recommended to face the active membrane layer that facilitates fouling materials removal by the combined physical/chemical cleaning. Spacers were also used for fouling mitigation, but experimental results demonstrated they could adversely impact membrane fouling (Hawari et al., 2018). The feed or draw solution pretreatment is the other method to reduce membrane fouling, maintaining a stable water flux (Hawari et al., 2018; Khanafer et al., 2021a). Despite the effectiveness of the pretreatment method for reducing membrane fouling, it increases the treatment cost. Overall, several methods are available for controlling and mitigating FO membrane fouling. Researchers also benefited from the RO membrane cleaning experience, made of the same chemicals in the FO membrane.

5. Draw Solution

The draw solution is the forward osmosis process's fundamental component and the source of its driving force. It is represented by the concentrated solution with a higher osmotic pressure to extract water from the feed across the membrane. The development of FO technology depends on the availability of an appropriate draw solution. Thus, much work has recently been put towards creating a novel draw solution that satisfies the following criteria: high water permeable flux, low reverse salt diffusion, low viscosity, fouling resistivity, chemical stability and compatibility with membrane, no toxicity, neutral pH, reasonably low cost and rapid recovery of the diluted draw solution with low energy requirements (Aende et al., 2020; Qin et al., 2012; Zhao et al., 2012). **Figure 4** presents the criterion and different categories of draw solutions used in the FO process, which are discussed in detail in the latter section.



(a)



(b)

Figure 4: a) draw solutions selection criteria, b) an overview of different types of draw solutions used in the FO process.

5.1. Draw solutions for the FO process.

5.1.1. Conventional organic ionic and inorganic solutions

Inorganic salts, including monovalent (NaCl , KCl , KBr , KNO_3 , NH_4Cl , KHCO_3 , NaHCO_3) and divalent salts (CaSO_4 , MgSO_4 , CuSO_4 , MgCl_2 , CaCl_2) have been the subject of the majority of investigations in the last few years. Due to their low cost, low molecular weight, high solubility, and strong osmotic pressure potential result in significant water flux and feed water recovery (Nguyen et al., 2015b, 2015a). It was noticeable that divalent and trivalent salts had lower reverse salt fluxes due to their larger hydrated radius and greater electrostatic repulsion than monovalent salts, which led to significant salt reverse leakages (Nguyen et al., 2015a). However, monovalent salt ions display higher water fluxes due to a higher diffusivity (Lutchmiah et al., 2014). Saline water is ubiquitous on Earth, making seawater a suitable and

626 affordable supply of DS. This abundance of saline water accounts for monovalent NaCl salt's
627 widespread use as draw solutes for various FO processes. NaCl is frequently used because
628 without the risk of scaling, it is easy to re-concentrate using the RO process, has a high-water
629 solubility, and exhibits high osmotic pressure characteristics that improve the performance of
630 FO operations (Akther et al., 2015). Notable examples include the study undertaken by
631 Hancock and Cath (2009), in which MgCl_2 was discovered to be a weaker DS due to the lower
632 osmotic pressure than NaCl; hence, the water flux obtained with MgCl_2 was 25–30% lower
633 than those obtained with NaCl DS. These results were confirmed by Ryan and co-workers
634 (2015), who found greater water flux was induced by NaCl draw solution but disagreed with
635 the findings by Jeng and Abdul Wahab (2017). In the latter study, researchers reported higher
636 water flux in the FO with MgCl_2 than with NaCl draw solution. A separate study simulated the
637 osmotic pressures of a range of osmotic agents using OLI Stream Analyzer software, indicating
638 the superior osmotic pressure of MgCl_2 compared to NaCl draw solution (Lutchmiah et al.,
639 2014). Besides, MgCl_2 showed a substantially slower RSF, 59–67%, probably due to the larger
640 molecular weight of magnesium ions. However, NaCl recovery methods, such as RO,
641 distillation, and electrodialysis, consume high energy (Li et al., 2020). Divalent MgSO_4 was
642 proposed for desalination because of its high solubility, availability and potential regeneration
643 by the NF membrane to reduce the regeneration cost (Al-Mayahi and Sharif, 2011; Sharif and
644 ARYAFAR, 2015). NF membranes of high Mg and SO_4 rejection, ~96%, and a water
645 permeability coefficient that would be several times larger than the RO membranes would
646 reduce the cost of MgSO_4 regeneration. Unfortunately, the low osmotic pressure of MgSO_4
647 requires a high concentration of DS for seawater desalination, which would increase reverse
648 salt diffusion and probably membrane fouling since Mg and SO_4 ions are precursors to
649 membrane fouling and scaling (Zhang et al., 2017). Also, NF regeneration of MgSO_4 DS

produces brackish water that requires further treatment for removal, increasing the number of filtration stages of the FO-NF system.

Contrarily, organic salts, which are described as any organic acid (anion) that has reacted with any inorganic or organic base (cation), was recently used as draw agent due to the lower accumulation of draw solute in feed side compared with inorganic draw solution (Al-Alalawy et al., 2017). In addition, higher salt rejection during the process of reverse osmosis reconcentration was another benefit for organic salts over their inorganic counterparts (Al-Alalawy et al., 2017). For example, organic phosphonate salts (OPSs) as novel draw solutes exhibited greater water flux and lower RSF than the conventional NaCl solution because of their higher osmotic pressure and lower viscosity (Long et al., 2016). This work also considered the NF process a successful recovery technique for diluted OPS solution after observing the rejection rates for all OPS solutions higher than 92% under the NF process (Long et al., 2016). The main disadvantage of organic DS agents is the potential to promote membrane biofouling; hence their application in the FO processes was limited. Also, the high viscosity of some organic draw solutions, e.g. sucrose, increases the ICP that would impact the water flux.

5.1.2. Functionalized nanoparticles (Magnetic nanoparticles, Na⁺-functionalized carbon quantum dots)

Magnetic nanoparticles (MNPs) are smart DS with an increased surface-to-volume ratio, and the surface functional groups can be tuned to change the osmotic pressure of the MNPs as DS (Tayel et al., 2020). MNPs have an osmotic pressure-producing capacity of roughly 70 atm, much higher than seawater's osmotic pressure of 26 atm, making them particularly desirable for desalination procedures (Akther et al., 2015; Ling and Chung, 2011). Additionally, due to their superparamagnetic characteristics, MNPs are sustainable that can be easily recovered and recycled using a straightforward external magnetic field without requiring chemical reaction or high energy consumption or through membrane processes such as nanofiltration (NF) or

675 microfiltration (MF) (Hafiz et al., 2022). Therefore, frequent use of these magnetic solutes
676 could significantly lower the cost of forward osmosis. Moreover, MNPs have a low RSF and
677 considerably bigger particle size than the membrane pores and organic and inorganic molecules
678 (Nguyen et al., 2015a; Tayel et al., 2020). In a study by Tayel et al. (2020), uncoated iron oxide
679 (Fe_3O_4) MNPs with 5 g% as DS showed a pure water flux of 35 LMH during the FO experiment
680 when DI was employed as the FS. Several studies indicated that MNPs could be modified using
681 nontoxic hydrophilic functional groups such as polymers (e.g. polyacrylic acid-PAA and
682 triethylene glycol-TREG), natural biopolymers (e.g. Chitosan, dextran, Gelatin, Sulfonated
683 sodium alginate and D-Xylose, Pectin) or other non-polymeric materials (e.g. Citrates and
684 Hydro-acids) as shell structures on the surface of the nanoparticles. This modification will
685 enhance their dispersity, stability in water and osmotic pressure in an aqueous solution as well
686 as decrease their particle size (Dey and Izake, 2015; Guizani et al., 2018; Hafiz et al., 2022; M.
687 Hafiz et al., 2021; Helix-Nielsen et al., 2022; Kim et al., 2020; M. Ling et al., 2011; Ling et al.,
688 2010; Ma et al., 2022; Na et al., 2014; Shoorangiz et al., 2022; Tayel et al., 2019). Nanoparticles
689 coated in polyacrylic acid were employed by Ling and Chung (2011) as the draw solute and DI
690 as the feed in the FO process. According to the findings, the osmotic pressure was 70 atm, and
691 the water flux was 17.5 LMH. While a 17.3 LMH water flow was produced in another
692 investigation using citrate-coated magnetic nanoparticles at a concentration of 20 mg/l as a DS
693 agent (Na et al., 2014; Shoorangiz et al., 2022). Also, low osmotic pressures, nanoparticle
694 aggregation, and inefficient separation are problems for magnetically responsive nanoparticles.
695 In aqueous solutions, magnetic nanoparticles tend to clump under a high-strength magnetic
696 field, significantly dropping the osmotic pressure and restricting their usefulness as FO solutes
697 (Amjad et al., 2018; Ma et al., 2022). For instance, Chung and colleagues found that the modest
698 particle aggregation in the high gradient magnetic field caused the average size of PAA-capped

magnetic nanoparticles to rise from 21 nm to 50.8 nm after recycling (Ling et al., 2010). As a result, in FO mode, the water flux decreased from 4 LMH to 3.6 LMH (Ling et al., 2010).

Similarly, after nine cycles, 79% of the starting flux was recovered by poly(ethylene glycol) diacid-coated magnetic particles. Their mean particle size rose from 13.5 nm to 19 nm (Ge et al., 2011). In response to this problem, Ling and Chung (2011), after each cycle, have ultrasonically redispersed agglomerated MNPs. The magnetic core of the MNPs eventually deteriorated after ultrasonication and lost some of their magnetic force, but the size of the MNPs was kept at its original value. To solve the MNP agglomeration issue, other regeneration techniques were also used. MNPs were recycled by Ling and Chung (2011) using UF instead of a strong magnetic field. MNPs larger than the UF membrane's pore size might seep through the membrane, whereas MNPs less than that size were prevented from agglomerating.

Another type of potential functionalized nanoparticle draw agents for FO has been explored using Na⁺ functionalized carbonized quantum dots (Na-CQDs) with an average size of 3.5 nm, which were made by heating citric acid powder in the air and then dispersing it in water with a pH-adjusted NaOH solution (Guo et al., 2014; Johnson et al., 2018). These hydrophilic CQDs produced exceptionally high osmotic pressures in their solutions, with a 0.5 g/L solution showing 5.7 MPa osmotic pressure, more than enough to overcome seawater's osmotic pressure (Guo et al., 2014). The CQDs' small size and the abundance of ions on their surfaces were thought to be the causes of their high osmotic pressure and well dispersion in water (Zhao et al., 2016). An initial water flux of 10.4 LMH was obtained when 0.4 g/ml of (Na-CQDs) was employed as a DS agent for FO desalination of seawater. After 5 test cycles, it marginally decreased to 9.6 LMH (Johnson et al., 2018).

The main drawbacks of magnetic nanoparticles could be summarized in the high fabrication cost compared to inorganic and organic salts, especially for desalination processes that require

a large volume draw solution. There are also concerns about the regeneration of magnetic nanoparticles as they tend to agglomerate during the regeneration process. The impact of nanoparticles on the environment and humans should be carefully scrutinized (Alejo et al., 2017). The main drawbacks of the Na-CQD draw solution are the preparation cost and high draw solution concentration requirements for seawater desalination (Yadav et al., 2020a). Na-CQD preparation involves citric acid heating at 180 °C, an energy-intensive process that increases the draw solution cost. Also, the suggested draw solution concentration for seawater water desalination is 4 g/mL or 400 g/L, which is extremely high.

5.1.3. Ionic liquids.

Ionic liquids (ILs) are salts with low melting points that can become liquid at low temperatures, usually below 100°C at atmospheric pressure (Dutta and Nath, 2018). ILs with the features of high water solubility, non-flammability, high ionization degree and good thermal and chemical stability have proven their great potential as draw solutes (Chen et al., 2019). For example, carboxylate-functionalized imidazolium ionic liquids (CFIMILs) as DS solute exhibited a negligible RSD with a water flux five times more than that of NaCl, and it was also entirely recycled using a membrane distillation (MD) process (Chen et al., 2019). Another utilized type of ionic liquids as potential draw solutes are the deep eutectic solvents (DES) that are referred to as bio ionic liquids such as Choline chloride-Ethylene glycol (Ch-Cl-EG) and Choline chloride – glycerol (Ch-Cl-glycerol) (Dutta and Nath, 2018). Their strong osmotic potential and ease of recovery have been demonstrated, improving the process's overall energy efficiency. DES, like Ethaline and Glycerine, have high osmotic pressure of around ($\pi \sim 365$ atm) and ($\pi \sim 317$ atm), respectively (Dutta and Nath, 2018). Furthermore, all the draw solutes based on IL and DES were reported to have poor RSF due to their high molecular weight. The main benefit of DES over IL is that they are simpler to manufacture and very

inexpensive to produce with high purity. The ionic liquid is a relatively new technology; hence, its toxicity and cost as a draw solution in the FO process should be assessed.

5.1.4. Thermolytic.

Ammonia carbonates, a thermolytic solution, are a viable DS for desalination applications (McCutcheon et al., 2006). Due to the good solubility in water and the high osmotic pressure of this DS, the flux was expected to be quite high. However, ICP negatively impacted process performance, and high RSF and biofouling were recorded due to the high diffusivity of ammonia (McCutcheon et al., 2006). For example, in a laboratory investigation, Hancock and Cath (2009) used CTA-FO membranes and NH_4HCO_3 as the draw solution to evaluate solute-coupled diffusion in the FO process. They discovered that NH_4HCO_3 had a much higher RSF than NaCl. For each litre of filtered water, 2,900 mg and 400 mg of NH_4HCO_3 and NaCl are lost from the DS. In contrast, it was found that simple heating can easily recover ammonia carbonates. It can be decomposed to ammonia and carbon dioxide gases at 60-65°C to produce freshwater (Lina, 2015; Qin et al., 2012). Ng et al. did a fundamental analysis of FO with an NH_4HCO_3 draw solution (Ng et al., 2006). Jiang et al. (2016) recovered freshwater from oil sand wastewater using a 4 mol/L (M) ammonium bicarbonate solution as DS. The rejection rate of ion pollutants was 80–100%, while the recovery rate was 85%. Besides, it was discovered that using ammonium bicarbonate in the forward osmosis membrane bioreactor (FO-MBR) was toxic for the microbial species (Gadelha et al., 2014). Several concerns were raised about thermolytic draw solutions, such as ammonia bicarbonate, including their high reverse diffusion, toxicity to humans and the environment, and residues in the product water. Also, reverse ammonium bicarbonate diffusion will contaminate the feed solution, e.g. seawater, causing additional environmental problems (Altaee, 2012).

5.1.5. Switchable polarity solvent (SPS)

SPS are mixtures of carbon dioxide, water, and tertiary amines and are examples of thermal-sensitive solutes (Stone et al., 2013; Wendt et al., 2015). The SPS FO method can handle extremely high-concentration solutions; it was already shown to produce positive FO water flux against a NaCl solution at 5 molal or 226,000 ppm total dissolved solids (TDS) (Stone et al., 2013). For instance, dimethylcyclohexylamine (DMCA), as SPS, was proposed by Stone and colleagues as the DS solute for the treatment of salt water, land-fill leachate, or industrial wastewater (Stone et al., 2013). Following the FO process, the SPS-containing high osmotic-pressure aqueous solution may transfer to the water and nonpolar liquid phases for separation. However, the heating and gas/vacuum required for this switching process consumes energy and raises the cost of the process. In addition, the problem of residual amine elimination is still open. Unquestionably, other significant problems that restrict the application of SPSs include material toxicity, expense, incompatibility with commercial FO membranes and chemical synthesis (Li and Wang, 2013; Stone et al., 2013). Despite these worries, SPS are still more cost-effective than pressure-driven processes like RO. Even with reduced energy efficiency, SPS FO is anticipated to have a cheap cost because heat energy costs are around ten times lower than the cost of electricity per unit of energy (Orme and Wilson, 2015; Wendt et al., 2015). According to calculations, the SPS FO process's overall equivalent energy needs for seawater desalination applications range from 2.4 to 4.3 kWh/m³ (depending on the degasser operating temperature) to dewater the solution to saturation (>90% water recovery). In comparison, the RO's specific power consumption ranges from 4 to 6 kWh/m³ for a ~50% water recovery (Wendt et al., 2015). Another effective type of SPS is 1-Cyclohexylpiperidine (CHP), which exhibits osmotic pressures (>500 atm) and flux performance comparable to that of (DMCA) while having significantly better material compatibility and degassing performance (Orme and Wilson, 2015). In addition, long-term stability was demonstrated by

the CHP-based DS and polyamide TFC membrane combination. RO was used to recover SPS DS; however, significant limitations included RSF and deterioration of the cellulose triacetate (CTA) membrane (Stone et al., 2013).

5.1.6. Thermo-responsive

The simplicity of thermally responsive draw solutes, the absence of additional chemicals, and the potential for using less expensive and environmentally friendly energy sources, such as geothermal, solar thermal energy and low-grade industrial waste heat, make them appeal (Cai et al., 2015a; Hsu et al., 2019). In addition, their easy recovery via simple temperature control makes them a good candidate for separating pure water from the draw solute. It is possible to use thermos-responsive draw solutes with either a lower critical solution temperature (LCST) or an upper critical solution temperature (UCST) characteristic (Ju et al., 2019). By manipulating the latter's solubility with temperature changes, these behaviours can separate pure water and the draw solute (Ju et al., 2019). Homopolymers, copolymers, oligomers, hydrogels, nanoparticles, and ionic liquids are just a few examples of the diverse types of thermo-responsive draw solutes with LCST and UCST characteristics studied by numerous researchers for the FO process (Abdullah et al., 2020; Cai et al., 2015b; Hartanto et al., 2015; Kim et al., 2014; Zhao et al., 2014b). For instance, thermally responsive ionic liquids have demonstrated greater efficacy in extracting water from feed streams with high salinity (Cai et al., 2015a; Zhong et al., 2016). In another work, the overall FO performance has increased using the hybrid ion liquid/hydrogel draw solution system by using the thermos-responsive features of both the ionic liquid (IL) and hydrogel. The hydrogel provides a convenient path to continuously and effectively regenerate water from the FO process and reduces the water flux decline of the IL as the DS agent (Hsu et al., 2019). Additionally, thermo-responsive microgels exhibited promising recyclability of water absorption and water recovery under the FO desalination process, attaining a water flux of up to 23.8 LMH and a

820 high-water recovery ability of up to 72.4% (Hartanto et al., 2015). Membrane distillation (MD)
821 was found to be an effective method to regenerate thermos-responsive copolymer DS agents
822 such as poly(sodiumstyrene-4-sulfonate-co-n-isopropylacrylamide) (PSSS-PNIPAM) and
823 produce clean water. This can happen by performing MD at a temperature above the LCST of
824 the copolymer, in which the DS's osmotic pressure decreases significantly due to polymer chain
825 agglomeration (Zhao et al., 2016).

826 Zhou et al. (2015) created magnetic thermally responsive nano-gels by coating magnetite
827 nanoparticles with the thermo-responsive copolymer poly(Nisopropylacrylamide-co-sodium
828 2-acrylamido-2-methylpropane sulfonate) (PNIPAM-co-AMPS). According to their findings,
829 the water flux increased 2.4 times compared to PAA-PNIPAM. These new thermo-responsive
830 MNPs could be easily trapped by either a low-strength magnetic field or UF membrane due to
831 the formed agglomerated larger particles when heated above the LCST (Han et al., 2013; Lina,
832 2015; M. M. Ling et al., 2011).

833 Polyelectrolytes and thermo-sensitive polyelectrolytes constitute novel class draw agents
834 with bright prospects due to their ability to dissolve in water and cause high osmotic pressure
835 and high-water fluxes in FO processes (Y. Wang et al., 2016). A thermo-sensitive poly(N-
836 isopropylacrylamide-co-acrylic acid) (PNA) polyelectrolyte is an example of thermo-sensitive
837 polyelectrolytes that offers high osmotic pressure and water flux by adjusting the pH value in
838 which the solubility and the ionization degree of its carboxyl groups can be raised (Y. Wang et
839 al., 2016). PNA can be recovered readily by either heating or centrifugation method. PNA-10
840 polyelectrolyte recovery percentages in both approaches can reach 89% (Y. Wang et al., 2016).
841 It is important also to note that more than 99.5% of the thermo-responsive polymer oligomeric
842 poly (tetrabutylphosphonium styrenesulfonate)s (PSSPs) have been recovered using only
843 thermal treatment (heating it above its LCST) without any additional membrane process or
844 appreciable reduction in the water permeation flux (14.50 LMH) (Kim et al., 2016). Geothermal

energy, biomass energy, and industrial waste heat are examples of low-grade heat sources that can provide thermal energy (above LCST) for these polymers (Kim et al., 2014). Another suggested low-energy polyelectrolyte recovery method is hot ultrafiltration (HUF), which recovered the water from polyelectrolyte DS by a 65.2% recovery fraction (Ou et al., 2013). Another study utilized the MF process after thermal precipitation to recover more than 99.7% of all polymer draw solutes with LCST (Kim et al., 2014).

5.1.7. Sol-gel.

Crosslinked polymers containing large volumes of water trapped within the three-dimensional network are known as hydrogels (Li et al., 2011a). Particularly, ionic group hydrogels on the comonomer unit can attract even higher water concentrations. Mobile counter ions balance the covalently integrated ionic groups. These counter ions create a positive osmotic pressure inside the hydrogel, which promotes higher water sorption and avoids reverse diffusion of the draw solute (Li et al., 2011a; Razmjou et al., 2013). It's significant to note that polymer hydrogels can alter in size in response to environmental factors like pH, temperature, electric fields, mechanical stress, antibodies, and more (Li et al., 2011b). Utilizing temperature, pressure, or solar irradiation (or a combination of these) as external stimuli are techniques by which polymer hydrogels can induce water to enter through the semipermeable membrane, and the water can then be released from swollen hydrogels (D. Li et al., 2013; Li et al., 2011a; Razmjou et al., 2013). A higher swelling ratio (pressure) causes the water and dewatering fluxes to be higher (D. Li et al., 2013). In a study by Li et al. (2011b), pure water was separated from swelling polymer hydrogels using sunlight irradiation as the stimulus. After 40 min exposure to the sunlight with 1.0 kW m^{-2} irradiation intensity, 100% water was recovered from swollen N, N- methylenebisacrylamide hydrogel containing light-absorbing carbon particles (PNI-PAM-C). The high viscosity of the sol-gel draw solution complicates their pumping and recirculations for large-volume desalination. Also, hydrogels require thermal processes for

regeneration, and swollen hydrogel pumping is impractical due to the high viscosity (Johnson et al., 2018).

5.1.8. Others

5.1.8.1. Dendrimers

Dendrimers are finely constructed spheroid or globular nanostructures that transport molecules enclosed in empty regions or bonded to the surface (Adham et al., 2007). Dendrimers' macromolecules offer high osmotic pressure; thus, they are a promising osmotic medium. According to preliminary UF investigations, the surface sodium ions were rejected by 87.3%, indicating that UF can reconcentrate the dendrimer and its surface ions (Adham et al., 2007). An example of a nontoxic and biocompatible dendrimer is poly(amidoamine) (PAMAM) which has a highly branched tree-like structure (Zhao et al., 2014a). The hyperbranched structure of PAMAM would permit lower solution viscosity than linear polyelectrolytes, resulting in a diminished negative impact of ICP on FO water flux (Hobson and Feast, 1999). PAMAM has a relatively high molecular size, which permits minimal RSF (Zhao et al., 2014a). In a laboratory investigation, Adham et al. (2007) identified dendrimers as potential DS with UF post-treatment and assessed the osmotic pressures of dendrimer solutions.

5.1.8.2. Fertilizers

Other non-potable uses of FO desalination, like irrigation and energy drinks, have a wide range of potential. Fertilizer-drawn forward osmosis (FDFO) desalination, in which fertilizers are employed as DS, was recently reported by Phuntsho et al. (Phuntsho et al., 2012a, 2011). The uniqueness of this specific FO procedure is that the desalinated, diluted DS, which contains vital plant nutrients, can be used immediately for fertigation. The separation and recovery of draw solutes needed when producing drinking water are no longer necessary with such a

technique. Therefore, using the FO process, energy consumption will be substantially lower than desalination for potable water (Phuntsho et al., 2012a).

Several studies have been conducted based on the FDFO process (Chekli et al., 2017; Zou and He, 2016). One kilogram of fertilizer was tested in 2011 as a DS for FO desalination, and it was shown to be capable of drawing 11 to 29 litres of water directly from seawater. The diluted fertilizer solution was then used for fertigation (Phuntsho et al., 2011). Zou and He (2016) claimed that 1 kg of fertilizer may remove 2459 L of freshwater from synthetic brackish water with high salinity. In addition, the use of FDFO for brackish water treatment has been demonstrated by Nasr and Sewilam (Nasr and Sewilam 2015). At the same time, El Zayat et al. (2021) investigated the concentration of artificial brine using an FDFO approach employing an industrial-grade $(\text{NH}_4)_2\text{SO}_4$. When using the DS and $(\text{NH}_4)_2\text{SO}_4$ with synthetic brine as the FS, the observed flux was 11.69 LMH. Another study recommended operating the process at a flux higher than 10 LMH to avoid loss of ammonium sulphate DS by reverse solute permeation (Nasr and Sewilam, 2016).

However, the concentration of fertilizer nutrients in the final FDFO product water, which may be higher than the acceptable nutrient limit for direct fertigation, was one of the restrictions found (Phuntsho et al., 2012b). A high fertilizer concentration would make the soil more saline and poisonous to plants. In that case, fresher water would be required to dilute the DS, which is undesirable. Other suggested possibilities to lower the nutrient concentration and make diluted DS acceptable for direct fertigation are using the NF process as a pre-treatment to lower TDS or post-treatment to partially recover the draw solute for reuse and recycling in subsequent processes (Phuntsho et al., 2012a). A recently established, successfully running, pilot-scale fertilizer-drawn forward osmosis and nanofiltration (FDFO-NF) system was operating for six months (Phuntsho et al., 2016). While utilizing blended fertilizers such as DS rather than single fertilizer could be another useful option to lower the nutrient concentration (Phuntsho et al.,

2012b). In addition, to lessen the damage of chemical fertilizers and increase soil fertility, organic fertilizers could be a potential approach, such as microalga *Spirulina* which was examined as DS in a study carried out by Al Bazedi et al. (2022).

Some drawbacks that might face the FDFO process are that NF is a pressure-driven membrane process. Using an additional process for the FDFO system will raise the system's energy consumption and, thus, the final cost of the produced water. For this reason, processes such as pressure-assisted forward osmosis (PAFO) were tested as a substitute approach to eliminate the need for NF post-treatment (Sahebi et al., 2015). This study found that using PAFO rather than NF could further dilute the fertilizer DS and produce permeate water that complied with the required nutrient concentrations for direct fertigation. In addition, RSF, rejection, and biofouling could be other significant issues for FDFO, as a fertilizer DS comprises nutrients containing N and P, which are considered precursors of biofouling in the FDFO desalination process in particular (Phuntsho et al., 2012a). Another drawback of fertilizer draw solution is the diffusion of N and P elements to the feed solution will contaminate the seawater, leading to algal bloom.

5.1.8.3. Surfactant/micellar as DS.

Above a specific critical concentration, organic and amphiphilic molecules in surfactant/micellar solutions can aggregate and be employed as draw solutions. Micellar solutes such as Triton X-100 (TX-100), cetylpyridinium chloride (CPC) and sodium dodecylsulfate (SDS) can produce a more consistent flux and much less RSF than inorganic salts while also attaining high levels of regeneration through UF (Gadelha et al., 2014; Roach et al., 2014). The low back diffusion of micellar solutions helps to prevent toxic contamination of the feed in wastewater treatment via FO-MBR (Gadelha et al., 2014). Another low-energy recovery method for micelles from diluted DS is the Kraft point method (Gadelha et al., 2014).

Lowering the solution temperature to a level below the Krafft temperature is a step in the Krafft point approach. Below this limit, micelles cannot develop; therefore, an excess of insoluble monomers produced by the initial micelles causes them to crystallize. Following crystallization, paper filtering is used to recover the surfactant. Surfactant recovery equals the amount of surfactant in the filtrate (Gadelha et al., 2014).

5.1.8.4. Concentrated seawater brines DS

One of the most significant and pressing environmental problems is disposing of concentrated brines from RO desalination plants containing concentrated organic and inorganic compounds. Therefore, in order to prevent any negative effects on the receiving environment, it is necessary to manage the RO concentrate sustainably. Recent research has, however, raised the possibility of using RO brines as a DS to address RO concentrate problems (Akther et al., 2015). A hybrid FO/RO process was developed by Bamaga et al. (2011) to reduce the risk of scaling during the desalination process by pre-treating the RO feed using the first FO procedure. RO brine is utilized as the DS for the second FO procedure to concentrate contaminated water and reduce its volume for further treatment. Therefore, the FO process is used in this application with RO brines as the DS to reduce the energy needed for desalination. The rejected brine from thermal desalination plants was used as a draw solution for seawater treatment and to benefit from the existing thermal plant for the draw solution regeneration (Khanafer et al., 2021a; Thabit et al., 2019). Bench-scale tests using real MSF brine and seawater achieved 22.3 L/m²h and 8.5% dilution of the draw solution at 40 °C brine temperature (Thabit et al., 2019). In another study, MSF brine was prepared by concentrating seawater as the draw solution in the FO process. The feed solution was tertiary sewage effluent (TSE) achieved 35 L/m²h water flux and a 43% reduction of the divalent ions in the solution (Khanafer et al., 2021a). Using TSE feed solution in the FO process achieved higher brine dilution than seawater feed solution and will reduce the capital and operating cost of the FO

967 process. The study also demonstrated a reversible FO fouling after cleaning with DI water only,
968 with 87.41% water recovery after 5 filtration cycles. One of the FO-MSF systems is that reverse
969 salt diffusion is not a problem since the draw solution is saline wastewater and the feed solution
970 is saline or wastewater.

971 Despite extensive efforts to find adequate draw agents for FO applications, as shown above,
972 the optimum candidates that can generate sufficient osmotic pressure and be entirely separated
973 from the water product at a cheap energy cost are difficult. **Figure 4** and **Table 5** describe the
974 main driving agents' benefits and drawbacks and the types and recovery techniques.

Draw solution	Examples	Pros	Cons	Recovery methods	References
Inorganic salts	Monovalent salts: NaCl, KCl, Divalent salts CaSO ₄ , MgSO ₄ , CuSO ₄ , MgCl ₂ , CaCl ₂	Low cost High solubility	Recovery is not often feasible ICP Clogging/scaling/fouling	RO NF Precipitation	(Aende et al., 2020; Akther et al., 2015; Johnson et al., 2018; Long et al., 2018)
Magnetic nanoparticles	Uncoated iron oxide (Fe ₃ O ₄) MNPs Polyacrylic acid-PAA- capped MNPs	High osmotic pressures at low concentrations No leakage Overcomes scaling and crystallisation issues in MD	Agglomeration during magnetic separation. Ultrasonication weakens magnetic properties. The viscosity of the solution reduces the effective driving force and the flux. Choice of a coating agent High molecular weights and low solubilities in water	Magnetic separation. UF Phase separation	(Blandin et al., 2020; Hafiz et al., 2022; Li and Wang, 2013; Ling et al., 2010; Long et al., 2018; Lutchmiah et al., 2014)
Carbon quantum dots (CQDs)	Na ⁺ -functionalized carbon quantum dots (Na-CQDs)	High osmotic pressure. Excellent dispersibility in water Low RSF. Biocompatibility and hydrophilicity Cheap precursor compounds.	Non- responsive. Issue of particle agglomeration.	MD	(Cai and Hu, 2016; Johnson et al., 2018; Long et al., 2018)
Ionic liquids	Imidazolium ionic liquids (IMILs) Carboxylate- functionalized imidazolium ionic liquids (CFIMILs) Deep eutectic solvents (DES) like Ethaline and Glyceline.	High water solubility High ionization degree Good stability. Low RSF	Cost.	Phase separation	(Chen et al., 2019; Long et al., 2018)
Thermolytic	Ammonium bicarbonate	High osmotic pressure	High RSD, Scaling precursor Insufficient removal of ammonia. Bad smell of ammonia. Requires heating Not thermally stable.	Moderate Heating	(Blandin et al., 2020; Long et al., 2018; McCutcheon et al., 2005)
SPSs	Dimethylcyclohexylamine (DMCA) 1-Cyclohexylpiperidine (CHP)	Energy efficient. High osmotic pressure.	Material toxicity Degrades the cellulose acetate membrane Poor water quality.	Heating	(Aende et al., 2020; Li and Wang, 2013; Qasim et al., 2015; Stone et al., 2013)
Thermo-responsive	Homopolymers. Copolymers (PSSS-PNIPAM) Oligomers. Hydrogels,	Simplicity Using less expensive and clean energy sources. Less chemicals usages	Drop in water flux due to agglomeration of MNPs Reverse salt flux. High viscosity. Complicated preparation.	Magnetic separation UF phase separation MD	(Johnson et al., 2018; Li and Wang, 2013;

Draw solution	Examples	Pros	Cons	Recovery methods	References
Thermo-sensitive polyelectrolytes	Nanoparticles. Ionic liquids	High osmotic pressure. Easy recovery	Some precursors are expensive.	Irradiating	Long et al., 2018)
	Poly (N-isopropylacrylamide-co-acrylic acid) (PNA) polyelectrolyte Poly acrylic acid sodium salts (PAA-Na) Poly (sodium 4-styrenesulfonate) (PSS)	High solubility. Cost-effective. Low energy requirement.	Low flux and poor water recovery Relatively high viscosity	Heating (Thermal precipitation) Centrifuging. UF	(Aende et al., 2020; Ge et al., 2013; Qasim et al., 2015)
Polymer hydrogels	N, N- methylenebisacrylamide hydrogel. poly(sodium acrylate)(PSA), poly(sodium acrylate)-co-poly(N-isopropyl acrylamide (PSA-NIPAM), poly(acrylamide) (PAM) and poly(N-isopropylacrylamide) (PNIPAM)	High water recovery	Energy intensive. Not suitable for practical applications. Microbial contamination is possible.	Direct application. Heating. Pressure stimuli	(Aende et al., 2020; Li et al., 2011a, 2011b; Qasim et al., 2015)
Dendrimers	poly(amidoamine) (PAMAM). Poly(amidoamine) terminated with sodium carboxylate groups (PAMAM-COONa)	High osmotic pressure and high-water flux.	UF and MD require energy pH-controlled removal is necessary Not feasible	Adjusting pH UF MD Crystallisation	(Aende et al., 2020; Qasim et al., 2015; Zhao et al., 2014a)
Fertilizers	Sulphate of ammonia (SOA) or (NH ₄) ₂ SO ₄ Ammonium chloride (NH ₄ Cl) KCl.	Absence of recovery process requirements. Relatively higher water flow rate.	High RSD. Potentially cost-intensive DS replacement Only applicable in agriculture.	Direct application	(Johnson et al., 2018)
Micellar solution	Triton X-100 (TX-100). Cetylpyridinium chloride (CPC). Sodium dodecylsulfate (SDS)	Low RSF Low energy recovery	Not feasible.	UF Krafft point	(Long et al., 2018)
Concentrated seawater brines	Brine	Reduce negative environmental effects.	Organic salt precipitation on the membrane surface	RO process	(Ling and Chung, 2011)

6. Pilot scale system

The viability of using simulated operations to treat saline and wastewater to produce potable (or superior) grade water necessitates pilot-scale system testing for FO-based desalination. Limited studies have proven the FO process's performance in a pilot-scale study, and most of these studies were conducted for a short period compared to the RO systems. In 2008, the Modern Water Company (MWC) investigated the first FO-RO pilot plant with a 18 m³/day capacity in Gibraltar for seawater desalination using manipulated draw solution of MgSO₄ (Nicoll, 2013; Thompson and Nicoll, 2011). The research scheme envisaged NF membrane application for the regeneration of the draw solution to reduce energy costs. Another full-scale commercial facility for Manipulated Osmosis Desalination (MOD) process was deployed with a capacity of (100 m³ /day) in the Al Wusta region of Oman (Nicoll, 2019; Thompson and Nicoll, 2011). The system consists of a FO system in a single cycle with a RO regeneration system to provide high-quality drinking water. The FO system was able to recover 35% of seawater. However, the system's optimum energy consumption evaluation with the impact of the energy recovery device is still needed (Thompson and Nicoll, 2011). Hafiz et al. (2023) assessed the feasibility of a pilot-scale FO process as a viable pre-treatment for a multi-stage flash (MSF) desalination plant regarding technical and economic aspects. This study used a commercial Toyobo's CTA hollow fibre FO membrane module to treat real seawater as FS and real MSF brine as DS. It was found that the FO process could resolve the scale problem in MSF desalination plants by achieving a high rejection rate of scaling ions (> 92%) with a low power consumption of 0.01 kWh/m³ (Hafiz et al., 2023). Additionally, in a study by Z. Wang et al. (2016), a pilot-scale FO system in Shanghai, China, concentrated real municipal wastewater using Hydration Technologies Innovation (HTI) CTA spiral-wound membrane module. The system showed a high phosphorus rejection rate of 99.7% and 48.1% rejection of ammonium. In another pilot investigation, two commercially available HF-FO modules were

tested for treating industrial wastewater from a gas production facility in Qatar (Minier-Matar et al., 2022). FO-RO pilot system was also used to treat raw produced water (PW) from the Denver-Julesburg basin (Colorado); the system rejected more than 99% of ions, although fouling was noted due to the organic constituents present in the PW (Maltos et al., 2018). The team determined that membrane cleaning and pre-treatment are required for the process to run well. Another pilot study of the osmotic dilution process used FO-RO to merge seawater desalination with municipal wastewater treatment utilizing a Porifera plate and frame membrane module (USA) (Zhan et al., 2021). The investigation aimed to comprehend and build a fouling index for the FO process that can be used to evaluate process performance and determine fouling and cleaning frequency.

Instead of RO as a DS recovery method, Ahmed et al. (2019) have utilized a thermal separation (TS) as a DS recovery method for using ethylene oxide-propylene oxide copolymer as a thermo-responsive DS in a 10 m³/day pilot plant of FO-TS system developed by Trevi Systems Inc. The FO pilot plant test unit is located at Desalination Research Plant (DRP) in Kuwait for desalinating Arabian Gulf seawater employing commercial scale hollow fibre (HF) FO membrane. The polyelectrolyte DS exhibited a high capability of producing substantial osmotic pressure differences in various compartments of the HF module, resulting in an average water recovery of 30% (Ahmed et al., 2019). Furthermore, Oasys examined the FO technique based on thermally recoverable ammonium carbonate DS and conducted a pilot study in the United States to treat high salinity PW (McGinnis et al., 2013). Electrodialysis (ED) method was also integrated with the FO system at a pilot scale test unit in Spain for landfill leachate (LL) concentration and draw and water recovery using Aquaporin's commercial FO hollow fibre modules (Sbardella et al., 2022). The FO system achieved 70% water recovery. However, the (FO-EDR) system's energy usage was relatively high, 8 kWh.m⁻³.

In contrast, the pilot-scale fertiliser-driven forward osmosis (FDFO) and nanofiltration (NF) system used for desalinating saline groundwater from coal mining activities in Australia has shown the feasibility of using the final water product for fertigation purposes (Phuntsho et al., 2016). A similar trend has been shown by coupling pilot-scale FDFO with hydroponic agriculture to desalinate brackish groundwater using a Porifera FO membrane module (Bassiouny et al., 2022). On the other hand, the impact of operating conditions such as flow rates and temperature on the FO pilot-scale system was considered in a study by Jalab et al. (2020) using Toyobo's commercial HF membrane. Future FO pilot tests should include the energy requirements for treatment, cost analysis, membrane fouling and mitigation methods for the long term to better understand the FO performance. Unfortunately, most studies were conducted for short terms, and the lack of commercial plant data makes the FO process less attractive regarding CAPEX and OPEX.

7. Implications

The key limitations for FO membranes include the impact of the ICP, permeability/selectivity trade-off, the swelling of the modified polymer, and complicated modification procedures. New advancements in membrane technologies allowed researchers to fabricate ultra-thin FO membranes of less than 200 μm structure parameter to alleviate the effect of concentration polarization. Numerous fabrication and modification techniques have been used to customize FO sublayers for FO systems. Most of these adjustments were made to improve the hydrophilicity, biocompatibility, and useful functioning of the FO membrane structure. Compared to phase inversion membranes, higher osmotic flux and lower structural parameter values were obtained for nanofiber membranes, making it a viable approach for manufacturing FO membranes.

On the other hand, TFC-based FO membranes provide more consistent water flux and specific reverse salt flux (SRSF). In addition, the favourable transport, physical, chemical, and biological properties of FO membranes have been proven to be improved by incorporating nanomaterials in synthesizing FO membranes. However, the agglomeration of the nanoparticles on the polymer matrix during the fabrication of nanocomposite membranes consider an important challenge. Therefore, different surface modifications of functional group-containing nanoparticles are favoured for consistent nanoparticle dispersion and nanoparticle loading concentrations. Compatibility and stability should be considered to prevent the leaching effect of nanomaterials in the environment.

The draw solution is still another crucial factor. An operation will greatly favour FO economics with a stream of high osmotic pressure that is readily available and does not require regeneration or recovery. Still, this will not be practicable in most circumstances, necessitating the implementation of draw type and recovery system selection. The ultimate concentration level required suitability for applications and the accompanying solution for draw recovery must be better considered when testing and choosing to draw solutions. Nonetheless, one of the disadvantages of DS regeneration is the significant energy consumption of pumping required for the downstream techniques such as RO, NF, MD, etc., and the high total cost of the operation, which also relies on the kind of DS utilized (Suwaileh et al., 2020). Therefore, it is crucial to create a suitable DS where the separation and recovery need less energy and where the draw solute can be profitably recycled and reused. Polyelectrolytes, responsive hydrogels, and nanoparticle-based systems are all examples of cutting-edge draw solutes. These are frequently big molecules or particles that can be concentrated again using high-flow filtration methods like UF or altering their physical characteristics to facilitate recovery through other methods. A minimal amount of energy will likely be required to re-concentrate any diluted DS since re-concentration necessitates that the osmotic potential of the DS maintains

its initial value (Ang et al., 2019). Also, additional research was carried out to identify circumstances in which low energy-based draw regeneration could be achieved. The studies included the application of fertilizers or soil treatments, in which the diluted DS can be utilized for additional applications, like fertigation, without requiring any regeneration process. However, the fertilizer DS could only draw water from a saline solution up to the concentration where the osmotic potentials of the FS and DS are equivalent. Besides, the final fertilizer content must be lowered to the permissible level for using water from various sources (Qin et al., 2012). It has long been thought that one of the sustainable solutions to the problem of high energy intensity, high operating cost, negating saltwater desalination systems regardless of the type of separation used, is to integrate FO systems for seawater desalination with renewable energy (solar thermal or wind power or geothermal energy or biomass power) or waste heat from industry (Aende et al., 2020; Suwaileh et al., 2020). Using these low-cost energy sources should be the main emphasis of future development on the draw solution. The main achievements and challenges reached in the FO process are listed in **Table 6**.

Membranes		Draw Solution	
Achievements	Challenges	Achievements	Challenges
CTA, CA, TFC, and TFN membranes were commercially developed for seawater and wastewater treatment. Membranes were tested for a short time, less than 5 years, in the laboratory, and pilot scales	Dimensions of the full-scale FO modules are not standardized yet compared to the RO/NF commercial membranes	A wide range of organic, inorganic, ionic liquids, magnetic nanoparticles and other draw solutions were developed for seawater and wastewater treatment	The concentrations of draw solution for seawater, brackish water, and wastewater are not standardized yet
High water flux and rejection rate FO membranes were fabricated commercially and in laboratory-scale	The cost of the FO membrane should be reduced. The cost of the FO membranes is ~10 times more than the RO membranes (Altaee et al., 2014).	Customized draw solutions were developed based on the end use and the regeneration process, such as thermolytic, fertilizer draw solutions etc.	The cost of the draw solution and environmental impact should be considered for newly developed products to justify their use, particularly for large capacity such as in seawater desalination
CP phenomenon was reduced in the new FO membranes with ultra-thin structure parameter	There is no standard method for FO membrane maintenance, and membrane cleaning and replacement should be documented similarly to that in the NF/RO systems		Reverse salt flux should consider the impact on the quality and safety of the feed solution in addition to membrane fouling. For example, elements like N and P are toxic to aquatic environments or a precursor for an algal bloom.
	More pilot plant tests are required to establish a database about the membrane lifetime, cleaning methods and long-term performance		

Table 6: Achievements and challenges reached in the FO process.

8. Conclusion

The review study has been conducted to evaluate and underline the progress and challenges in the FO process modelling, membrane fabrication and the draw solution. Undoubtedly, there is evident progress in the FO process modelling and simulation for permeation and reverse salt flux prediction. External and internal concentration polarization and external membrane resistance in the FO models made these models more powerful in the design of experimental works. A wide range of draw solutions are proposed for the FO process, but only a few are suitable for large-capacity applications. A successful draw solution should be inexpensive, available, easy to use and regenerate, non-toxic, and possess elevated osmotic pressure. The contamination of feed solution due to reverse salt flux should be addressed in selecting draw solutions, especially for the draw solutions containing toxic compounds. Future FO desalination systems might benefit from solutes that can be easily regenerated with minimal energy. The potential of draw solutes to create much higher osmotic pressure than typical ones would be crucial in increasing production. On the other hand, the small molecule/ion size of the draw solute can increase reverse salt diffusion. As a result, minimizing the reverse mobility of draw solute while maintaining high water permeable flux is a critical area that can open up new potential for FO desalination in the future. New FO membranes designed with a small structure parameter can reduce the effects of concentration polarization, achieving high water flux. Membranes with low structural parameters, a highly selective active layer, and chemically and mechanically stable are desirable to ensure minimal concentration polarization, high water flux and insignificant reverse salt flux. The main challenge in the FO membrane is the membrane cost, which is high for commercial applications. Despite the many conducted studies of FO membrane fabrication and draw solute type effect, further cost analyses, pilot scale tests,

1114 and full module tests must be performed instead of flat sheet lab tests to avoid the inconsistency
1115 between the simulation study and the bench scale experiments.

1116 Acknowledgements:

1117 This project is supported by the Drought Resilience through funding from the Australian
1118 Government's Future Drought Fund.

1119 **References:**

1120 Ab Hamid, N.H., Ye, L., Wang, D.K., Smart, S., Filloux, E., Lebouteiller, T., Zhang, X.,
1121 2018. Evaluating the membrane fouling formation and chemical cleaning strategy in
1122 forward osmosis membrane filtration treating domestic sewage. Environmental Science:
1123 Water Research and Technology 4, 2092–2103. <https://doi.org/10.1039/c8ew00584b>

1124 Abdullah, M.A.M., Man, M.S., Abdullah, S.B., Saufi, S.M., 2020. Synthesis and
1125 characterization of thermo-responsive ionic liquids (TRILs). IOP Conference Series:
1126 Materials Science and Engineering 736. [https://doi.org/10.1088/1757-](https://doi.org/10.1088/1757-899X/736/4/042027)
1127 [899X/736/4/042027](https://doi.org/10.1088/1757-899X/736/4/042027)

1128 Abounahia, N., Qiblawey, H., Zaidi, S.J., 2022. Progress for Co-Incorporation of
1129 Polydopamine and Nanoparticles for Improving Membranes Performance. Membranes
1130 12, 1–32. <https://doi.org/10.3390/membranes12070675>

1131 Adham, S., Oppenheimer, J., Liu, L., Kumar, M., 2007. Dewatering reverse osmosis
1132 concentrate from water reuse using forward osmosis, WateReuse Foundation Research
1133 Report, Product No. 05-009-01.

1134 Aende, A., Gardy, J., Hassanpour, A., 2020. Seawater desalination: A review of forward
1135 osmosis technique, its challenges, and future prospects. Processes 8.
1136 <https://doi.org/10.3390/PR8080901>

1137 Ahmed, D., Isawi, H., Badway, N., Elbayaa, A., Shawky, H., 2021. Highly porous cellulosic
 1138 nanocomposite membranes with enhanced performance for forward osmosis
 1139 desalination. *Iranian Polymer Journal (English Edition)* 30, 423–444.
 1140 <https://doi.org/10.1007/s13726-021-00901-4>

1141 Ahmed, D.F., Isawi, H., Badway, N.A., Elbayaa, A.A., Shawky, H., 2021. Graphene oxide
 1142 incorporated cellulose triacetate/cellulose acetate nanocomposite membranes for
 1143 forward osmosis desalination. *Arabian Journal of Chemistry* 14, 102995.
 1144 <https://doi.org/10.1016/j.arabjc.2021.102995>

1145 Ahmed, M., Kumar, R., Garudachari, B., Thomas, J.P., 2019. Assessment of pilot scale
 1146 forward osmosis system for Arabian Gulf seawater desalination using polyelectrolyte
 1147 draw solution. *Desalination and Water Treatment* 157, 342–348.
 1148 <https://doi.org/10.5004/dwt.2019.24267>

1149 Ahn, H.R., Tak, T.M., Kwon, Y.N., 2015. Preparation and applications of poly vinyl alcohol
 1150 (PVA) modified cellulose acetate (CA) membranes for forward osmosis (FO) processes.
 1151 *Desalination and Water Treatment* 53, 1–7.
 1152 <https://doi.org/10.1080/19443994.2013.834516>

1153 Akther, N., Sodiq, A., Giwa, A., Daer, S., Arafat, H.A., Hasan, S.W., 2015. Recent
 1154 advancements in forward osmosis desalination: A review. *Chemical Engineering Journal*
 1155 281, 502–522. <https://doi.org/10.1016/j.cej.2015.05.080>

1156 Al-Alalawy, A.F., Abbas, T.R., Mohammed, H.K., 2017. Comparative Study for Organic and
 1157 Inorganic Draw Solutions in Forward Osmosis. *Al-Khwarizmi Engineering Journal* 13,
 1158 94–102. <https://doi.org/10.22153/kej.2017.08.007>

1159 Al-Mayahi, A., Sharif, A., 2011. (12) United States Patent.

1160 Al Bazed, G., Soliman, N., Sewilam, H., 2022. Novel organic draw solution in forward
 1161 osmosis process for fertigation: performance evaluation and flux prediction.
 1162 Environmental Science and Pollution Research 29, 68881–68891.
 1163 <https://doi.org/10.1007/s11356-022-20674-4>

1164 Alejo, T., Arruebo, M., Carcelen, V., Monsalvo, V.M., Sebastian, V., 2017. Advances in
 1165 draw solutes for forward osmosis: Hybrid organic-inorganic nanoparticles and
 1166 conventional solutes. Chemical Engineering Journal 309, 738–752.
 1167 <https://doi.org/10.1016/j.cej.2016.10.079>

1168 Alfahel, R., Azzam, R.S., Hafiz, M.A., Hawari, A.H., Pandey, R.P., Mahmoud, K.A., Hassan,
 1169 M.K., Elzatahry, A.A., 2020. Fabrication of fouling resistant Ti3C2Tx
 1170 (MXene)/cellulose acetate nanocomposite membrane for forward osmosis application.
 1171 Journal of Water Process Engineering 38, 101551.
 1172 <https://doi.org/10.1016/j.jwpe.2020.101551>

1173 Alihemati, Z., Hashemifard, S.A., Matsuura, T., Ismail, A.F., Hilal, N., 2020. Current status
 1174 and challenges of fabricating thin film composite forward osmosis membrane: A
 1175 comprehensive roadmap. Desalination 491, 114557.
 1176 <https://doi.org/10.1016/j.desal.2020.114557>

1177 Altaee, A., 2012. Forward osmosis: Potential use in desalination and water treatment. Journal
 1178 of Membrane and Separation Technology 1, 79–93. [https://doi.org/10.6000/1929-](https://doi.org/10.6000/1929-6037.2012.01.02.2)
 1179 [6037.2012.01.02.2](https://doi.org/10.6000/1929-6037.2012.01.02.2)

1180 Altaee, A., Alanezi, A.A., Hawari, A.H., 2018. Forward osmosis feasibility and potential
 1181 future application for desalination, Emerging Technologies for Sustainable Desalination
 1182 Handbook. Elsevier Inc. <https://doi.org/10.1016/B978-0-12-815818-0.00002-3>

1183 Altaee, A., Sharif, A., 2014. Pressure retarded osmosis: Advancement in the process

1184 applications for power generation and desalination. *Desalination* 356, 31–46.
 1185 <https://doi.org/10.1016/j.desal.2014.09.028>

1186 Altaee, A., Zaragoza, G., Drioli, E., Zhou, J., 2017. Evaluation the potential and energy
 1187 efficiency of dual stage pressure retarded osmosis process. *Applied Energy* 199, 359–
 1188 369. <https://doi.org/10.1016/j.apenergy.2017.05.031>

1189 Altaee, A., Zaragoza, G., Sharif, A., 2014. Pressure retarded osmosis for power generation
 1190 and seawater desalination: Performance analysis. *Desalination* 344, 108–115.
 1191 <https://doi.org/10.1016/j.desal.2014.03.022>

1192 Amini, M., Jahanshahi, M., Rahimpour, A., 2013. Synthesis of novel thin film
 1193 nanocomposite (TFN) forward osmosis membranes using functionalized multi-walled
 1194 carbon nanotubes. *Journal of Membrane Science* 435, 233–241.
 1195 <https://doi.org/10.1016/j.memsci.2013.01.041>

1196 Amjad, M., Gardy, J., Hassanpour, A., Wen, D., 2018. Novel draw solution for forward
 1197 osmosis based solar desalination. *Applied Energy* 230, 220–231.
 1198 <https://doi.org/10.1016/j.apenergy.2018.08.021>

1199 Ang, W.L., Wahab Mohammad, A., Johnson, D., Hilal, N., 2019. Forward osmosis research
 1200 trends in desalination and wastewater treatment: A review of research trends over the
 1201 past decade. *Journal of Water Process Engineering* 31, 100886.
 1202 <https://doi.org/10.1016/j.jwpe.2019.100886>

1203 Bagherzadeh, M., Nikkhoo, M., Ahadian, M.M., Amini, M., 2023. Novel Thin-Film
 1204 Nanocomposite Forward Osmosis Membranes Modified with WS₂/CuAl LDH
 1205 Nanocomposite to Enhance Desalination and Anti-fouling Performance. *Journal of*
 1206 *Inorganic and Organometallic Polymers and Materials*. [https://doi.org/10.1007/s10904-](https://doi.org/10.1007/s10904-023-02547-6)
 1207 [023-02547-6](https://doi.org/10.1007/s10904-023-02547-6)

1208 Bamaga, O.A., Yokochi, A., Zabara, B., Babaqi, A.S., 2011. Hybrid FO/RO desalination
 1209 system: Preliminary assessment of osmotic energy recovery and designs of new FO
 1210 membrane module configurations. *Desalination* 268, 163–169.
 1211 <https://doi.org/10.1016/j.desal.2010.10.013>

1212 Baniasadi, J., Shabani, Z., Mohammadi, T., Sahebi, S., 2021. Enhanced performance and
 1213 fouling resistance of cellulose acetate forward osmosis membrane with the spatial
 1214 distribution of TiO₂ and Al₂O₃ nanoparticles, *Journal of Chemical Technology and*
 1215 *Biotechnology*. <https://doi.org/10.1002/jctb.6521>

1216 Bassiouny, M., Nasr, P., Sewilam, H., 2022. Investigating the pilot-scale performance of a
 1217 hydroponic nutrient solution as potential draw solution for fertilizer drawn forward
 1218 osmosis and hydroponic agriculture of lettuce. *Clean Technologies and Environmental*
 1219 *Policy* 24, 2749–2760. <https://doi.org/10.1007/s10098-022-02349-3>

1220 Blandin, G., Ferrari, F., Lesage, G., Le-Clech, P., Hérán, M., Martinez-Lladó, X., 2020.
 1221 Forward osmosis as concentration process: Review of opportunities and challenges.
 1222 *Membranes* 10, 1–40. <https://doi.org/10.3390/membranes10100284>

1223 Bui, N.N., Lind, M.L., Hoek, E.M.V., McCutcheon, J.R., 2011. Electrospun nanofiber
 1224 supported thin film composite membranes for engineered osmosis. *Journal of Membrane*
 1225 *Science* 385–386, 10–19. <https://doi.org/10.1016/j.memsci.2011.08.002>

1226 Cai, Y., Hu, X.M., 2016. A critical review on draw solutes development for forward osmosis.
 1227 *Desalination* 391, 16–29. <https://doi.org/10.1016/j.desal.2016.03.021>

1228 Cai, Y., Shen, W., Wei, J., Chong, T.H., Wang, R., Krantz, W.B., Fane, A.G., Hu, X., 2015a.
 1229 Energy-efficient desalination by forward osmosis using responsive ionic liquid draw
 1230 solutes. *Environmental Science: Water Research and Technology* 1, 341–347.
 1231 <https://doi.org/10.1039/c4ew00073k>

- 1232 Cai, Y., Wang, R., Krantz, W.B., Fane, A.G., Hu, X., 2015b. Exploration of using thermally
1233 responsive polyionic liquid hydrogels as draw agents in forward osmosis. RSC
1234 Advances 5, 97143–97150. <https://doi.org/10.1039/c5ra19018e>
- 1235 Cath, T.Y., Elimelech, M., McCutcheon, J.R., McGinnis, R.L., Achilli, A., Anastasio, D.,
1236 Brady, A.R., Childress, A.E., Farr, I. V., Hancock, N.T., Lampi, J., Nghiem, L.D., Xie,
1237 M., Yip, N.Y., 2013. Standard Methodology for Evaluating Membrane Performance in
1238 Osmotically Driven Membrane Processes. Desalination 312, 31–38.
1239 <https://doi.org/10.1016/j.desal.2012.07.005>
- 1240 Chandran, A.M., Tayal, E., Mural, P.K.S., 2022. Polycaprolactone-blended cellulose acetate
1241 thin-film composite membrane for dairy waste treatment using forward osmosis.
1242 Environmental Science and Pollution Research. [https://doi.org/10.1007/s11356-022-](https://doi.org/10.1007/s11356-022-20813-x)
1243 20813-x
- 1244 Chaoui, I., Ndiaye, I., Abderafi, S., Vaudreuil, S., Bounahmidi, T., 2021. Evaluation of fo
1245 membranes performance using a modelling approach. Desalination and Water Treatment
1246 223, 71–98. <https://doi.org/10.5004/dwt.2021.27132>
- 1247 Chekli, L., Kim, Y., Phuntsho, S., Li, S., Ghaffour, N., Leiknes, T.O., Shon, H.K., 2017.
1248 Evaluation of fertilizer-drawn forward osmosis for sustainable agriculture and water
1249 reuse in arid regions. Journal of Environmental Management 187, 137–145.
1250 <https://doi.org/10.1016/j.jenvman.2016.11.021>
- 1251 Chen, G.E., Sun, W.G., Wu, Q., Kong, Y.F., Xu, Z.L., Xu, S.J., Zheng, X.P., 2017. Effect of
1252 cellulose triacetate membrane thickness on forward-osmosis performance and
1253 application for spent electroless nickel plating baths. Journal of Applied Polymer
1254 Science 134, 1–10. <https://doi.org/10.1002/app.45049>
- 1255 Chen, Q., Ge, Q., Xu, W., Pan, W., 2019. Functionalized imidazolium ionic liquids promote

1256 seawater desalination through forward osmosis. *Journal of Membrane Science* 574, 10–
 1257 16. <https://doi.org/10.1016/j.memsci.2018.11.078>

1258 Chen, X., Xu, J., Lu, J., Shan, B., Gao, C., 2017. Enhanced performance of cellulose
 1259 triacetate membranes using binary mixed additives for forward osmosis desalination.
 1260 *Desalination* 405, 68–75. <https://doi.org/10.1016/j.desal.2016.12.003>

1261 Chia, W.Y., Khoo, K.S., Chia, S.R., Chew, K.W., Yew, G.Y., Ho, Y.C., Show, P.L., Chen,
 1262 W.H., 2020. Factors affecting the performance of membrane osmotic processes for
 1263 bioenergy development. *Energies* 13. <https://doi.org/10.3390/en13020481>

1264 Chiao, Y.H., Sengupta, A., Chen, S.T., Huang, S.H., Hu, C.C., Hung, W.S., Chang, Y., Qian,
 1265 X., Wickramasinghe, S.R., Lee, K.R., Lai, J.Y., 2019. Zwitterion augmented polyamide
 1266 membrane for improved forward osmosis performance with significant antifouling
 1267 characteristics. *Separation and Purification Technology* 212, 316–325.
 1268 <https://doi.org/10.1016/j.seppur.2018.09.079>

1269 Choi, H.G., Son, M., Yoon, S.H., Celik, E., Kang, S., Park, H., Park, C.H., Choi, H., 2015.
 1270 Alginate fouling reduction of functionalized carbon nanotube blended cellulose acetate
 1271 membrane in forward osmosis. *Chemosphere* 136, 204–210.
 1272 <https://doi.org/10.1016/j.chemosphere.2015.05.003>

1273 Chun, Y., Mulcahy, D., Zou, L., Kim, I.S., 2017. A short review of membrane fouling in
 1274 forward osmosis processes. *Membranes* 7, 1–23.
 1275 <https://doi.org/10.3390/membranes7020030>

1276 Chung, T.S., Li, X., Ong, R.C., Ge, Q., Wang, H., Han, G., 2012. Emerging forward osmosis
 1277 (FO) technologies and challenges ahead for clean water and clean energy applications.
 1278 *Current Opinion in Chemical Engineering* 1, 246–257.
 1279 <https://doi.org/10.1016/j.coche.2012.07.004>

1280 Dabaghian, Z., Rahimpour, A., 2015. Carboxylated carbon nanofibers as hydrophilic porous
 1281 material to modification of cellulosic membranes for forward osmosis desalination.
 1282 Chemical Engineering Research and Design 104, 647–657.
 1283 <https://doi.org/10.1016/j.cherd.2015.10.008>

1284 Deng, L., Wang, Q., An, X., Li, Z., Hu, Y., 2020. Towards enhanced antifouling and flux
 1285 performances of thin-film composite forward osmosis membrane via constructing a
 1286 sandwich-like carbon nanotubes-coated support. Desalination 479, 114311.
 1287 <https://doi.org/10.1016/j.desal.2020.114311>

1288 Dey, P., Izake, E.L., 2015. Magnetic nanoparticles boosting the osmotic efficiency of a
 1289 polymeric FO draw agent: Effect of polymer conformation. Desalination 373, 79–85.
 1290 <https://doi.org/10.1016/j.desal.2015.07.010>

1291 Ding, J., Sarrigani, G.V., Khan, H.J., Yang, H., Sohimi, N.A., Izzati Sukhairul Zaman, N.Z.,
 1292 Zhong, X., Mai-Prochnow, A., Wang, D.K., 2020. Designing Hydrogel-Modified
 1293 Cellulose Triacetate Membranes with High Flux and Solute Selectivity for Forward
 1294 Osmosis. Industrial and Engineering Chemistry Research 59, 20845–20853.
 1295 <https://doi.org/10.1021/acs.iecr.0c03977>

1296 Dsilva Winfred Rufuss, D., Kapoor, V., Arulvel, S., Davies, P.A., 2022. Advances in forward
 1297 osmosis (FO) technology for enhanced efficiency and output: A critical review. Journal
 1298 of Cleaner Production 356, 131769. <https://doi.org/10.1016/j.jclepro.2022.131769>

1299 Duong, P.H.H., Nunes, S.P., Chung, T.S., 2016. Dual-skinned polyamide/poly(vinylidene
 1300 fluoride)/cellulose acetate membranes with embedded woven. Journal of Membrane
 1301 Science 520, 840–849. <https://doi.org/10.1016/j.memsci.2016.08.047>

1302 Dutta, S., Nath, K., 2018. Prospect of ionic liquids and deep eutectic solvents as new
 1303 generation draw solution in forward osmosis process. Journal of Water Process

1304 Engineering 21, 163–176. <https://doi.org/10.1016/j.jwpe.2017.12.012>

1305 El-Noss, M., Isawi, H., Shawky, H.A., Gomaa, M.A., Abdel-Mottaleb, M.S.A., 2020.

1306 Improvement of cellulose acetate forward osmosis membrane performance using zinc

1307 oxide nanoparticles. *Desalination and Water Treatment* 193, 19–33.

1308 <https://doi.org/10.5004/dwt.2020.25677>

1309 El Zayat, H., Nasr, P., Sewilam, H., 2021. Investigating sustainable management of

1310 desalination brine through concentration using forward osmosis. *Environmental Science*

1311 and *Pollution Research* 28, 39938–39951. <https://doi.org/10.1007/s11356-021-13311-z>

1312 Emadzadeh, D., Lau, W.J., Matsuura, T., Rahbari-Sisakht, M., Ismail, A.F., 2014. A novel

1313 thin film composite forward osmosis membrane prepared from PSf-TiO₂ nanocomposite

1314 substrate for water desalination. *Chemical Engineering Journal* 237, 70–80.

1315 <https://doi.org/10.1016/j.cej.2013.09.081>

1316 Gadelha, G., Nawaz, M.S., Hankins, N.P., Khan, S.J., Wang, R., Tang, C.Y., 2014.

1317 Assessment of micellar solutions as draw solutions for forward osmosis. *Desalination*

1318 354, 97–106. <https://doi.org/10.1016/j.desal.2014.09.009>

1319 Ge, Q., Ling, M., Chung, T.S., 2013. Draw solutions for forward osmosis processes:

1320 Developments, challenges, and prospects for the future. *Journal of Membrane Science*

1321 442, 225–237. <https://doi.org/10.1016/j.memsci.2013.03.046>

1322 Ge, Q., Su, J., Chung, T.S., Amy, G., 2011. Hydrophilic superparamagnetic nanoparticles:

1323 Synthesis, characterization, and performance in forward osmosis processes. *Industrial*

1324 and *Engineering Chemistry Research* 50, 382–388. <https://doi.org/10.1021/ie101013w>

1325 Ghaemi, N., Khodakarami, Z., 2019. Nano-biopolymer effect on forward osmosis

1326 performance of cellulosic membrane: High water flux and low reverse salt.

- 1327 Carbohydrate Polymers 204, 78–88. <https://doi.org/10.1016/j.carbpol.2018.10.005>
- 1328 Ghosh, B., Ghosh, A.K., Bindal, R.C., Tewari, P.K., 2015. Studies on Concentration of
 1329 Simulated Ammonium-diuranate Filtered Effluent Solution by Forward Osmosis Using
 1330 Indigenously Developed Cellulosic Osmosis Membranes. Separation Science and
 1331 Technology (Philadelphia) 50, 324–331. <https://doi.org/10.1080/01496395.2014.973517>
- 1332 Guizani, M., Maeda, T., Ito, R., Funamizu, N., 2018. Synthesis and characterization of
 1333 magnetic nanoparticles as a candidate draw solution for forward osmosis. Journal of
 1334 Water and Environment Technology 16, 63–71. <https://doi.org/10.2965/jwet.17-040>
- 1335 Guo, C.X., Zhao, D., Zhao, Q., Wang, P., Lu, X., 2014. Na⁺-functionalized carbon quantum
 1336 dots: A new draw solute in forward osmosis for seawater desalination. Chemical
 1337 Communications 50, 7318–7321. <https://doi.org/10.1039/c4cc01603c>
- 1338 Hadadpour, S., Tavakol, I., Shabani, Z., Mohammadi, T., Tofighy, M.A., Sahebi, S., 2021.
 1339 Synthesis and characterization of novel thin film composite forward osmosis membrane
 1340 using charcoal-based carbon nanomaterials for desalination application. Journal of
 1341 Environmental Chemical Engineering 9, 104880.
 1342 <https://doi.org/10.1016/j.jece.2020.104880>
- 1343 Hafiz, M., Hassanein, A., Talhami, M., AL-Ajji, M., Hassan, M.K., Hawari, A.H., 2022.
 1344 Magnetic nanoparticles draw solution for forward osmosis: current status and future
 1345 challenges in wastewater treatment. Journal of Environmental Chemical Engineering 10,
 1346 108955. <https://doi.org/10.1016/j.jece.2022.108955>
- 1347 Hafiz, M., Talhami, M., Ba-Abbad, M.M., Hawari, A.H., 2021. Optimization of magnetic
 1348 nanoparticles draw solution for high water flux in forward osmosis. Water (Switzerland)
 1349 13. <https://doi.org/10.3390/w13243653>

- 1350 Hafiz, M.A., Alfahel, R., Altaee, A., Hawari, A.H., 2023. Techno-economic assessment of
1351 forward osmosis as a pretreatment process for mitigation of scaling in multi-stage flash
1352 seawater desalination process. *Separation and Purification Technology* 309, 123007.
1353 <https://doi.org/10.1016/j.seppur.2022.123007>
- 1354 Hafiz, M.A., Hawari, A.H., Alfahel, R., Hassan, M.K., Altaee, A., 2021. Comparison of
1355 nanofiltration with reverse osmosis in reclaiming tertiary treated municipal wastewater
1356 for irrigation purposes. *Membranes* 11, 1–13.
1357 <https://doi.org/10.3390/membranes11010032>
- 1358 Han, G., Chung, T.S., Toriida, M., Tamai, S., 2012. Thin-film composite forward osmosis
1359 membranes with novel hydrophilic supports for desalination. *Journal of Membrane*
1360 *Science* 423–424, 543–555. <https://doi.org/10.1016/j.memsci.2012.09.005>
- 1361 Han, H., Lee, J.Y., Lu, X., 2013. Thermoresponsive nanoparticles + plasmonic nanoparticles
1362 = photoresponsive heterodimers: Facile synthesis and sunlight-induced reversible
1363 clustering. *Chemical Communications* 49, 6122–6124.
1364 <https://doi.org/10.1039/c3cc42273a>
- 1365 Han, J.C., Xing, X.Y., Wang, J., Wu, Q.Y., 2022. Preparation and Properties of Thin-Film
1366 Composite Forward Osmosis Membranes Supported by Cellulose Triacetate Porous
1367 Substrate via a Nonsolvent-Thermally Induced Phase Separation Process. *Membranes*
1368 12. <https://doi.org/10.3390/membranes12040412>
- 1369 Hancock, N.T., Cath, T.Y., 2009. Solute coupled diffusion in osmotically driven membrane
1370 processes. *Environmental Science and Technology* 43, 6769–6775.
1371 <https://doi.org/10.1021/es901132x>
- 1372 Hartanto, Y., Yun, S., Jin, B., Dai, S., 2015. Functionalized thermo-responsive microgels for
1373 high performance forward osmosis desalination. *Water Research* 70, 385–393.

1374 <https://doi.org/10.1016/j.watres.2014.12.023>

1375 Hawari, A.H., Al-Qahoumi, A., Ltaief, A., Zaidi, S., Altaee, A., 2018. Dilution of seawater
 1376 using dewatered construction water in a hybrid forward osmosis system. *Journal of*
 1377 *Cleaner Production* 195, 365–373. <https://doi.org/10.1016/j.jclepro.2018.05.211>

1378 Helix-nielsen, C., Vohl, S., Stergar, J., 2022. Synthesis of magnetic nanoparticles with
 1379 covalently bonded polyacrylic acid for use as forward osmosis draw agents.
 1380 *Environmental Science Water Research & Technology*.
 1381 <https://doi.org/10.1039/d2ew00539e>

1382 Hobson, L.J., Feast, W.J., 1999. Poly(amidoamine) hyperbranched systems: Synthesis,
 1383 structure and characterization. *Polymer* 40, 1279–1297. [https://doi.org/10.1016/S0032-](https://doi.org/10.1016/S0032-3861(98)00268-7)
 1384 [3861\(98\)00268-7](https://doi.org/10.1016/S0032-3861(98)00268-7)

1385 Holloway, R.W., Maltos, R., Vanneste, J., Cath, T.Y., 2015. Mixed draw solutions for
 1386 improved forward osmosis performance. *Journal of Membrane Science* 491, 121–131.
 1387 <https://doi.org/10.1016/j.memsci.2015.05.016>

1388 Hoover, L.A., Schiffman, J.D., Elimelech, M., 2013. Nanofibers in thin-film composite
 1389 membrane support layers: Enabling expanded application of forward and pressure
 1390 retarded osmosis. *Desalination* 308, 73–81. <https://doi.org/10.1016/j.desal.2012.07.019>

1391 Hsu, C.H., Ma, C., Bui, N., Song, Z., Wilson, A.D., Kostecki, R., Diederichsen, K.M.,
 1392 McCloskey, B.D., Urban, J.J., 2019. Enhanced forward osmosis desalination with a
 1393 hybrid ionic liquid/hydrogel thermoresponsive draw agent system. *ACS Omega* 4,
 1394 4296–4303. <https://doi.org/10.1021/acsomega.8b02827>

1395 Ibrar, I., Altaee, A., Zhou, J.L., Naji, O., Khanafer, D., 2020a. Challenges and potentials of
 1396 forward osmosis process in the treatment of wastewater. *Critical Reviews in*

1397 Environmental Science and Technology 50, 1339–1383.

1398 <https://doi.org/10.1080/10643389.2019.1657762>

1399 Ibrar, I., Khanafer, D., Yadav, S., Bakly, S., Ali, J., n.d. DESALINATION BY FORWARD

1400 OSMOSIS : FAILURE , SUCCESS ,.

1401 Ibrar, I., Naji, O., Sharif, A., Malekizadeh, A., Alhawari, A., Alanezi, A.A., Altaee, A., 2019.

1402 A review of fouling mechanisms, control strategies and real-time fouling monitoring

1403 techniques in forward osmosis. Water (Switzerland) 11.

1404 <https://doi.org/10.3390/w11040695>

1405 Ibrar, I., Yadav, S., Altaee, A., Hawari, A., Nguyen, V., Zhou, J., 2020b. A novel empirical

1406 method for predicting concentration polarization in forward osmosis for single and

1407 multicomponent draw solutions. Desalination 494, 114668.

1408 <https://doi.org/10.1016/j.desal.2020.114668>

1409 Ibrar, I., Yadav, S., Altaee, A., Safaei, J., Akshaya K. Samal, Senthilmurugan Subbiah, G.M.,

1410 Deka, P., Zhou, J., 2022a. Sodium docusate as a cleaning agent for forward osmosis

1411 membrane s fouled by landfill leachate wastewater. Chemosphere 136237.

1412 <https://doi.org/https://doi.org/10.1016/j.chemosphere.2022.136237>

1413 Ibrar, I., Yadav, S., Altaee, A., Samal, A.K., Zhou, J.L., Nguyen, T.V., Ganbat, N., 2020c.

1414 Treatment of biologically treated landfill leachate with forward osmosis: Investigating

1415 membrane performance and cleaning protocols. Science of the Total Environment 744,

1416 140901. <https://doi.org/10.1016/j.scitotenv.2020.140901>

1417 Ibrar, I., Yadav, S., Braytee, A., Altaee, A., HosseinZadeh, A., Samal, A.K., Zhou, J.L.,

1418 Khan, J.A., Bartocci, P., Fantozzi, F., 2022b. Evaluation of machine learning algorithms

1419 to predict internal concentration polarization in forward osmosis. Journal of Membrane

1420 Science 646, 120257. <https://doi.org/10.1016/j.memsci.2022.120257>

- 1421 Ibrar, I., Yadav, S., Ganbat, N., Samal, A.K., Altaee, A., Zhou, J.L., Nguyen, T.V., 2021.
 1422 Feasibility of H₂O₂ cleaning for forward osmosis membrane treating landfill leachate.
 1423 Journal of Environmental Management 294, 113024.
 1424 <https://doi.org/https://doi.org/10.1016/j.jenvman.2021.113024>
- 1425 Ibrar, I., Yadav, S., Naji, O., Alanezi, A.A., Ghaffour, N., Déon, S., Subbiah, S., Altaee, A.,
 1426 2022c. Development in forward Osmosis-Membrane distillation hybrid system for
 1427 wastewater treatment. Separation and Purification Technology 286.
 1428 <https://doi.org/10.1016/j.seppur.2022.120498>
- 1429 Im, S.J., Viet, N.D., Jang, A., 2021. Real-time monitoring of forward osmosis membrane
 1430 fouling in wastewater reuse process performed with a deep learning model.
 1431 Chemosphere 275, 130047. <https://doi.org/10.1016/j.chemosphere.2021.130047>
- 1432 Jain, H., Dhupper, R., Verma, A.K., Garg, M.C., 2021. Development of titanium dioxide
 1433 incorporated ultrathin cellulose acetate membrane for enhanced forward osmosis
 1434 performance. Nanotechnology for Environmental Engineering 6, 1–8.
 1435 <https://doi.org/10.1007/s41204-021-00161-w>
- 1436 Jain, H., Verma, A.K., Dhupper, R., Wadhwa, S., Garg, M.C., 2022. Development of CA-
 1437 TiO₂-incorporated thin-film nanocomposite forward osmosis membrane for enhanced
 1438 water flux and salt rejection. International Journal of Environmental Science and
 1439 Technology 19, 5387–5400. <https://doi.org/10.1007/s13762-021-03415-x>
- 1440 Jalab, R., Awad, A.M., Nasser, M.S., Minier-Matar, J., Adham, S., 2020. Pilot-scale
 1441 investigation of flowrate and temperature influence on the performance of hollow fiber
 1442 forward osmosis membrane in osmotic concentration process. Journal of Environmental
 1443 Chemical Engineering 8, 104494. <https://doi.org/10.1016/j.jece.2020.104494>
- 1444 Jamil, T.S., Nasr, R.A., Abbas, H.A., Ragab, T.I.M., Xabela, S., Mutloali, R., 2022. Low-

1445 Cost High Performance Polyamide Thin Film Composite (Cellulose Triacetate/Graphene
1446 Oxide) Membranes for Forward Osmosis Desalination from Palm Fronds. *Membranes*
1447 12. <https://doi.org/10.3390/membranes12010006>

1448 Jawad, J., Hawari, A.H., Zaidi, S., 2020. Modeling of forward osmosis process using artificial
1449 neural networks (ANN) to predict the permeate flux. *Desalination* 484, 114427.
1450 <https://doi.org/10.1016/j.desal.2020.114427>

1451 Jeng Yih Law, Abdul Wahab Mohammad, 2017. ASSESSING THE FORWARD OSMOSIS
1452 PERFORMANCES USING CTA MEMBRANE: EFFECT OF SOLUTION VOLUME
1453 RATIO AND TYPE OF DRAW SOLUTE. *Jurnal Teknologi* 3, 47–52.
1454 <https://doi.org/10.11113/jt.v79.11326>

1455 Jiang, Y., Liang, J., Liu, Y., 2016. Application of forward osmosis membrane technology for
1456 oil sands process-affected water desalination. *Water Science and Technology* 73, 1809–
1457 1816. <https://doi.org/10.2166/wst.2016.014>

1458 Jin, H., Huang, Y., Wang, X., Yu, P., Luo, Y., 2016. Preparation of modified cellulose
1459 acetate membranes using functionalized multi-walled carbon nanotubes for forward
1460 osmosis. *Desalination and Water Treatment* 57, 7166–7174.
1461 <https://doi.org/10.1080/19443994.2015.1017010>

1462 Johnson, D.J., Suwaileh, W.A., Mohammed, A.W., Hilal, N., 2018. Osmotic ' s potential : An
1463 overview of draw solutes for forward osmosis G R A P H I C A L A B S T R A C T.
1464 *Desalination* 434, 100–120.

1465 Ju, C., Park, C., Kim, T., Kang, S., Kang, H., 2019. Thermo-responsive draw solute for
1466 forward osmosis process; Poly(ionic liquid) having lower critical solution temperature
1467 characteristics. *RSC Advances* 9, 29493–29501. <https://doi.org/10.1039/c9ra04020j>

1468 K, A., Mungray, A., Agarwal, S., Ali, J., Chandra Garg, M., 2021. Performance optimisation
 1469 of forward-osmosis membrane system using machine learning for the treatment of
 1470 textile industry wastewater. *Journal of Cleaner Production* 289, 125690.
 1471 <https://doi.org/10.1016/j.jclepro.2020.125690>

1472 Kahrizi, M., Gonzales, R.R., Kong, L., Matsuyama, H., Lu, P., Lin, J., Zhao, S., 2022.
 1473 Significant roles of substrate properties in forward osmosis membrane performance: A
 1474 review. *Desalination* 528, 115615. <https://doi.org/10.1016/j.desal.2022.115615>

1475 Khanafer, D., Ibrahim, I., Yadav, S., Altaee, A., Hawari, A., Zhou, J., 2021a. Brine reject
 1476 dilution with treated wastewater for indirect desalination. *Journal of Cleaner Production*
 1477 322, 129129. <https://doi.org/10.1016/j.jclepro.2021.129129>

1478 Khanafer, D., Yadav, S., Ganbat, N., Altaee, A., Zhou, J., Hawari, A.H., 2021b. Performance
 1479 of the pressure assisted forward osmosis-msf hybrid desalination plant. *Water*
 1480 (Switzerland) 13, 1–16. <https://doi.org/10.3390/w13091245>

1481 Kim, C., Lee, J., Schmucker, D., Fortner, J.D., 2020. Highly stable superparamagnetic iron
 1482 oxide nanoparticles as functional draw solutes for osmotically driven water transport.
 1483 *npj Clean Water* 3, 1–6. <https://doi.org/10.1038/s41545-020-0055-9>

1484 Kim, J. joo, Chung, J.S., Kang, H., Yu, Y.A., Choi, W.J., Kim, H.J., Lee, J.C., 2014. Thermo-
 1485 responsive copolymers with ionic group as novel draw solutes for forward osmosis
 1486 processes. *Macromolecular Research* 22, 963–970. [https://doi.org/10.1007/s13233-014-](https://doi.org/10.1007/s13233-014-2142-6)
 1487 [2142-6](https://doi.org/10.1007/s13233-014-2142-6)

1488 Kim, J., Park, K., Yang, D.R., Hong, S., 2019. A comprehensive review of energy
 1489 consumption of seawater reverse osmosis desalination plants. *Applied Energy* 254,
 1490 113652. <https://doi.org/10.1016/j.apenergy.2019.113652>

1491 Kim, J.J., Kang, H., Choi, Y.S., Yu, Y.A., Lee, J.C., 2016. Thermo-responsive oligomeric
 1492 poly(tetrabutylphosphonium styrenesulfonate)s as draw solutes for forward osmosis
 1493 (FO) applications. *Desalination* 381, 84–94. <https://doi.org/10.1016/j.desal.2015.11.013>

1494 Kumar, R., Ahmed, M., Garudachari, B., Thomas, J.P., 2018. Evaluation of the Forward
 1495 Osmosis Performance of Cellulose Acetate Nanocomposite Membranes. *Arabian*
 1496 *Journal for Science and Engineering* 43, 5871–5879. [https://doi.org/10.1007/s13369-](https://doi.org/10.1007/s13369-017-3048-3)
 1497 [017-3048-3](https://doi.org/10.1007/s13369-017-3048-3)

1498 Lakra, R., Balakrishnan, M., Basu, S., 2021. Development of cellulose acetate-chitosan-metal
 1499 organic framework forward osmosis membrane for recovery of water and nutrients from
 1500 wastewater. *Journal of Environmental Chemical Engineering* 9, 105882.
 1501 <https://doi.org/10.1016/j.jece.2021.105882>

1502 Lee, K.L., Baker, R.W., Lonsdale, H.K., 1981. Membranes for power generation by pressure-
 1503 retarded osmosis. *Journal of Membrane Science* 8, 141–171.
 1504 [https://doi.org/10.1016/S0376-7388\(00\)82088-8](https://doi.org/10.1016/S0376-7388(00)82088-8)

1505 Lee, W.J., Ng, Z.C., Hubadillah, S.K., Goh, P.S., Lau, W.J., Othman, M.H.D., Ismail, A.F.,
 1506 Hilal, N., 2020. Fouling mitigation in forward osmosis and membrane distillation for
 1507 desalination. *Desalination* 480. <https://doi.org/10.1016/j.desal.2020.114338>

1508 Li, D., Wang, H., 2013. Smart draw agents for emerging forward osmosis application.
 1509 *Journal of Materials Chemistry A* 1, 14049–14060. <https://doi.org/10.1039/c3ta12559a>

1510 Li, D., Zhang, X., Simon, G.P., Wang, H., 2013. Forward osmosis desalination using polymer
 1511 hydrogels as a draw agent: Influence of draw agent, feed solution and membrane on
 1512 process performance. *Water Research* 47, 209–215.
 1513 <https://doi.org/10.1016/j.watres.2012.09.049>

- 1514 Li, D., Zhang, X., Yao, J., Simon, G.P., Wang, H., 2011a. Stimuli-responsive polymer
1515 hydrogels as a new class of draw agent for forward osmosis desalination. *Chemical*
1516 *Communications* 47, 1710–1712. <https://doi.org/10.1039/c0cc04701e>
- 1517 Li, D., Zhang, X., Yao, J., Zeng, Y., Simon, G.P., Wang, H., 2011b. Composite polymer
1518 hydrogels as draw agents in forward osmosis and solar dewatering. *Soft Matter* 7,
1519 10048–10056. <https://doi.org/10.1039/c1sm06043k>
- 1520 Li, F., Sun, M., Cheng, Q., Yang, B., 2016. Preparation and Characterization of Graphene
1521 Oxide / Cellulose Triacetate Forward Osmosis Membranes. *MATEC Web of*
1522 *Conferences* 67. <https://doi.org/10.1051/matecconf/20166701015>
- 1523 Li, G., Li, X.M., He, T., Jiang, B., Gao, C., 2013. Cellulose triacetate forward osmosis
1524 membranes: Preparation and characterization. *Desalination and Water Treatment* 51,
1525 2656–2665. <https://doi.org/10.1080/19443994.2012.749246>
- 1526 Li, G., Wang, J., Hou, D., Bai, Y., Liu, H., 2015. Fabrication and performance of PET mesh
1527 enhanced cellulose acetate membranes for forward osmosis. *Journal of Environmental*
1528 *Sciences (China)* 45, 7–17. <https://doi.org/10.1016/j.jes.2015.11.025>
- 1529 Li, L., Shi, W., Yu, S., 2020. Research on forward osmosis membrane technology still needs
1530 improvement in water recovery and wastewater treatment. *Water (Switzerland)* 12, 1–
1531 27. <https://doi.org/10.3390/w12010107>
- 1532 Li, T., Ba, X., Wang, X., Wang, Z., Yang, J., Cui, Y., Wang, L., 2022a. MIL-53(Fe)@ γ -
1533 Al_2O_3 nanocomposites incorporated cellulose acetate for forward osmosis membranes
1534 of high desalination performance. *Environmental Engineering Research* 28, 210448–0.
1535 <https://doi.org/10.4491/eer.2021.448>
- 1536 Li, T., Cheng, C., Zhang, K., Yang, J., Han, G., Wang, X., Wang, Z., Wang, L., 2022b. UiO-

1537 66-NH₂ nanocomposites incorporated cellulose acetate for forward osmosis membranes
 1538 of high desalination performance. *Environmental Technology (United Kingdom)* 0, 1–
 1539 12. <https://doi.org/10.1080/09593330.2022.2099306>

1540 Li, T., Wang, Y., Wang, Xinyan, Cheng, C., Zhang, K., Yang, J., Han, G., Wang, Z., Wang,
 1541 Xiuju, Wang, L., 2022c. Desalination Characteristics of Cellulose Acetate FO
 1542 Membrane Incorporated with ZIF-8 Nanoparticles. *Membranes* 12.
 1543 <https://doi.org/10.3390/membranes12020122>

1544 Li, X., Wang, K.Y., Helmer, B., Chung, T.S., 2012. Thin-film composite membranes and
 1545 formation mechanism of thin-film layers on hydrophilic cellulose acetate propionate
 1546 substrates for forward osmosis processes. *Industrial and Engineering Chemistry*
 1547 *Research* 51, 10039–10050. <https://doi.org/10.1021/ie2027052>

1548 Lin, X., He, Y., Zhang, Y., Yu, W., Lian, T., 2021. Sulfonated covalent organic frameworks
 1549 (COFs) incorporated cellulose triacetate/cellulose acetate (CTA/CA)-based mixed
 1550 matrix membranes for forward osmosis. *Journal of Membrane Science* 638, 119725.
 1551 <https://doi.org/10.1016/j.memsci.2021.119725>

1552 Lina, 2015. DEVELOPING MULTIFUNCTIONAL FORWARD OSMOSIS (FO) DRAW
 1553 SOLUTES FOR SEAWATER DESALINATION. NATIONAL UNIVERSITY OF
 1554 SINGAPORE.

1555 Ling, M., Chung, T.-S., Wang, K., Ge, Q., Su, J., 2011. Forward osmosis process using
 1556 hydrophilic magnetic nanoparticles as draw solutes. *PCT Int. Appl.*

1557 Ling, M.M., Chung, T.S., 2011. Desalination process using super hydrophilic nanoparticles
 1558 via forward osmosis integrated with ultrafiltration regeneration. *Desalination* 278, 194–
 1559 202. <https://doi.org/10.1016/j.desal.2011.05.019>

1560 Ling, M.M., Chung, T.S., Lu, X., 2011. Facile synthesis of thermosensitive magnetic
 1561 nanoparticles as “smart” draw solutes in forward osmosis. *Chemical Communications*
 1562 47, 10788–10790. <https://doi.org/10.1039/c1cc13944d>

1563 Ling, M.M., Wang, K.Y., Chung, T.S., 2010. Highly Water-Soluble Magnetic Nanoparticles
 1564 as Novel Draw Solutes in Forward Osmosis for Water Reuse. *Industrial and Engineering*
 1565 *Chemistry Research* 49, 5869–5876.

1566 Liu, X., Wu, J., Hou, L. an, Wang, J., 2020. Fouling and cleaning protocols for forward
 1567 osmosis membrane used for radioactive wastewater treatment. *Nuclear Engineering and*
 1568 *Technology* 52, 581–588. <https://doi.org/10.1016/j.net.2019.08.007>

1569 Long, Q., Jia, Y., Li, J., Yang, J., Liu, F., Zheng, J., Yu, B., 2018. Recent advance on draw
 1570 solutes development in Forward osmosis. *Processes* 6, 7–11.
 1571 <https://doi.org/10.3390/pr6090165>

1572 Long, Q., Shen, L., Chen, R., Huang, J., Xiong, S., Wang, Y., 2016. Synthesis and
 1573 Application of Organic Phosphonate Salts as Draw Solutes in Forward Osmosis for Oil-
 1574 Water Separation. *Environmental Science and Technology* 50, 12022–12029.
 1575 <https://doi.org/10.1021/acs.est.6b02953>

1576 Lu, P., Liang, S., Qiu, L., Gao, Y., Wang, Q., 2016. Thin film nanocomposite forward
 1577 osmosis membranes based on layered double hydroxide nanoparticles blended
 1578 substrates. *Journal of Membrane Science* 504, 196–205.
 1579 <https://doi.org/10.1016/j.memsci.2015.12.066>

1580 Lutchmiah, K., Verliefde, A.R.D., Roest, K., Rietveld, L.C., Cornelissen, E.R., 2014.
 1581 Forward osmosis for application in wastewater treatment: A review. *Water Research* 58,
 1582 179–197. <https://doi.org/10.1016/j.watres.2014.03.045>

1583 Ma, D., Tian, Y., He, T., Zhu, X., 2022. Preparation of novel magnetic nanoparticles as draw
 1584 solutes in forward osmosis desalination. *Chinese Journal of Chemical Engineering* 46,
 1585 223–230. <https://doi.org/10.1016/j.cjche.2021.07.013>

1586 Madsen, H.T., Nissen, S.S., Muff, J., Søgaaard, E.G., 2017. Pressure retarded osmosis from
 1587 hypersaline solutions: Investigating commercial FO membranes at high pressures.
 1588 *Desalination* 420, 183–190. <https://doi.org/10.1016/j.desal.2017.06.028>

1589 Maiti, S., Samantaray, P.K., Bose, S., 2020. In situ assembly of a graphene oxide quantum
 1590 dot-based thin-film nanocomposite supported on de-mixed blends for desalination
 1591 through forward osmosis. *Nanoscale Advances* 2, 1993–2003.
 1592 <https://doi.org/10.1039/c9na00688e>

1593 Maltos, R.A., Regnery, J., Almaraz, N., Fox, S., Schutter, M., Cath, T.J., Veres, M., Coday,
 1594 B.D., Cath, T.Y., 2018. Produced water impact on membrane integrity during extended
 1595 pilot testing of forward osmosis – reverse osmosis treatment. *Desalination* 440, 99–110.
 1596 <https://doi.org/10.1016/j.desal.2018.02.029>

1597 Manickam, S.S., McCutcheon, J.R., 2017. Understanding mass transfer through asymmetric
 1598 membranes during forward osmosis: A historical perspective and critical review on
 1599 measuring structural parameter with semi-empirical models and characterization
 1600 approaches, *Desalination*. <https://doi.org/10.1016/j.desal.2016.12.016>

1601 McCutcheon, J.R., Elimelech, M., 2006. Influence of concentrative and dilutive internal
 1602 concentration polarization on flux behavior in forward osmosis. *Journal of Membrane*
 1603 *Science* 284, 237–247. <https://doi.org/10.1016/j.memsci.2006.07.049>

1604 McCutcheon, J.R., McGinnis, R.L., Elimelech, M., 2006. Desalination by ammonia-carbon
 1605 dioxide forward osmosis: Influence of draw and feed solution concentrations on process
 1606 performance. *Journal of Membrane Science* 278, 114–123.

1607 <https://doi.org/10.1016/j.memsci.2005.10.048>

1608 McCutcheon, J.R., McGinnis, R.L., Elimelech, M., 2005. A novel ammonia-carbon dioxide
1609 forward (direct) osmosis desalination process. *Desalination* 174, 1–11.
1610 <https://doi.org/10.1016/j.desal.2004.11.002>

1611 McGinnis, R.L., Hancock, N.T., Nowosielski-Slepowron, M.S., McGurgan, G.D., 2013. Pilot
1612 demonstration of the NH₃/CO₂ forward osmosis desalination process on high salinity
1613 brines. *Desalination* 312, 67–74. <https://doi.org/10.1016/j.desal.2012.11.032>

1614 Minier-Matar, J., Al-Maas, M., Hussain, A., Nasser, M.S., Adham, S., 2022. Pilot-scale
1615 evaluation of forward osmosis membranes for volume reduction of industrial
1616 wastewater. *Desalination* 531, 115689. <https://doi.org/10.1016/j.desal.2022.115689>

1617 Mirkhalili, S.M., Mousavi, S.A., Saadat Abadi, A.R., Sadeghi, M., 2017. Preparation of
1618 mesh-reinforced cellulose acetate forward osmosis membrane with very low surface
1619 roughness. *Korean Journal of Chemical Engineering* 34, 3170–3177.
1620 <https://doi.org/10.1007/s11814-017-0206-y>

1621 Na, Y., Yang, S., Lee, S., 2014. Evaluation of citrate-coated magnetic nanoparticles as draw
1622 solute for forward osmosis. *Desalination* 347, 34–42.
1623 <https://doi.org/10.1016/j.desal.2014.04.032>

1624 Nagy, E., 2014. A general, resistance-in-series, salt- and water flux models for forward
1625 osmosis and pressure-retarded osmosis for energy generation. *Journal of Membrane*
1626 *Science* 460, 71–81. <https://doi.org/10.1016/j.memsci.2014.02.021>

1627 Nasr, P., Sewilam, H., 2016. Investigating the performance of ammonium sulphate draw
1628 solution in fertilizer drawn forward osmosis process. *Clean Technologies and*
1629 *Environmental Policy* 18, 717–727. <https://doi.org/10.1007/s10098-015-1042-6>

1630 Nasr, P., Sewilam, H., 2015. The potential of groundwater desalination using forward
 1631 osmosis for irrigation in Egypt. *Clean Technologies and Environmental Policy* 17,
 1632 1883–1895. <https://doi.org/10.1007/s10098-015-0902-4>

1633 Ng, H.Y., Tang, W., Wong, W.S., 2006. Performance of forward (direct) osmosis process:
 1634 Membrane structure and transport phenomenon. *Environmental Science and Technology*
 1635 40, 2408–2413. <https://doi.org/10.1021/es0519177>

1636 Nguyen, H.T., Chen, S.S., Nguyen, N.C., Ngo, H.H., Guo, W., Li, C.W., 2015a. Exploring an
 1637 innovative surfactant and phosphate-based draw solution for forward osmosis
 1638 desalination. *Journal of Membrane Science* 489, 212–219.
 1639 <https://doi.org/10.1016/j.memsci.2015.03.085>

1640 Nguyen, H.T., Nguyen, N.C., Chen, S.S., Ngo, H.H., Guo, W., Li, C.W., 2015b. A new class
 1641 of draw solutions for minimizing reverse salt flux to improve forward osmosis
 1642 desalination. *Science of the Total Environment* 538, 129–136.
 1643 <https://doi.org/10.1016/j.scitotenv.2015.07.156>

1644 Nguyen, T.P.N., Yun, E.T., Kim, I.C., Kwon, Y.N., 2013. Preparation of cellulose
 1645 triacetate/cellulose acetate (CTA/CA)-based membranes for forward osmosis. *Journal of*
 1646 *Membrane Science* 433, 49–59. <https://doi.org/10.1016/j.memsci.2013.01.027>

1647 Nicoll, P., 2013. Forward Osmosis is not to be Ignored. *Desalination & Water Reuse* 22, 5.

1648 Nicoll, P.G., 2019. Forward Osmosis - A brief introduction FORWARD OSMOSIS – A
 1649 BRIEF INTRODUCTION. *The International Desalination Association World Congress*
 1650 *on Desalination and Water Reuse* 2013 1.

1651 Orme, C.J., Wilson, A.D., 2015. 1-Cyclohexylpiperidine as a thermolytic draw solute for
 1652 osmotically driven membrane processes. *Desalination* 371, 126–133.

1653 <https://doi.org/10.1016/j.desal.2015.05.024>

1654 Ou, R., Wang, Y., Wang, H., Xu, T., 2013. Thermo-sensitive polyelectrolytes as draw
1655 solutions in forward osmosis process. *Desalination* 318, 48–55.
1656 <https://doi.org/10.1016/j.desal.2013.03.022>

1657 Pan, S.F., Dong, Y., Zheng, Y.M., Zhong, L. Bin, Yuan, Z.H., 2017. Self-sustained
1658 hydrophilic nanofiber thin film composite forward osmosis membranes: Preparation,
1659 characterization and application for simulated antibiotic wastewater treatment. *Journal*
1660 of *Membrane Science* 523, 205–215. <https://doi.org/10.1016/j.memsci.2016.09.045>

1661 Park, M.J., Phuntsho, S., He, T., Nisola, G.M., Tijing, L.D., Li, X.M., Chen, G., Chung, W.J.,
1662 Shon, H.K., 2015. Graphene oxide incorporated polysulfone substrate for the fabrication
1663 of flat-sheet thin-film composite forward osmosis membranes. *Journal of Membrane*
1664 *Science* 493, 496–507. <https://doi.org/10.1016/j.memsci.2015.06.053>

1665 Phillip, W.A., Schiffman, J.D., Elimelech, M., 2010. High Performance Thin-Film
1666 Membrane. *Environmental Science and Technology* 44, 3812–3818.

1667 Phuntsho, S., Kim, J.E., Johir, M.A.H., Hong, S., Li, Z., Ghaffour, N., Leiknes, T.O., Shon,
1668 H.K., 2016. Fertiliser drawn forward osmosis process: Pilot-scale desalination of mine
1669 impaired water for fertigation. *Journal of Membrane Science* 508, 22–31.
1670 <https://doi.org/10.1016/j.memsci.2016.02.024>

1671 Phuntsho, S., Shon, H.K., Hong, S., Lee, S., Vigneswaran, S., 2011. A novel low energy
1672 fertilizer driven forward osmosis desalination for direct fertigation: Evaluating the
1673 performance of fertilizer draw solutions. *Journal of Membrane Science* 375, 172–181.
1674 <https://doi.org/10.1016/j.memsci.2011.03.038>

1675 Phuntsho, S., Shon, H.K., Hong, S., Lee, S., Vigneswaran, S., Kandasamy, J., 2012a.

1676 Fertiliser drawn forward osmosis desalination: The concept, performance and limitations
 1677 for fertigation. *Reviews in Environmental Science and Biotechnology* 11, 147–168.
 1678 <https://doi.org/10.1007/s11157-011-9259-2>

1679 Phuntsho, S., Shon, H.K., Majeed, T., El Saliby, I., Vigneswaran, S., Kandasamy, J., Hong,
 1680 S., Lee, S., 2012b. Blended fertilizers as draw solutions for fertilizer-drawn forward
 1681 osmosis desalination. *Environmental Science and Technology* 46, 4567–4575.
 1682 <https://doi.org/10.1021/es300002w>

1683 Qasim, M., Darwish, N.A., Sarp, S., Hilal, N., 2015. Water desalination by forward (direct)
 1684 osmosis phenomenon: A comprehensive review. *Desalination* 374, 47–69.
 1685 <https://doi.org/10.1016/j.desal.2015.07.016>

1686 Qiao, Z., Wang, Z., Zhang, C., Yuan, S., Zhu, Y., Wang, J., 2012. Developing Thin-Film-
 1687 Composite Forward Osmosis Membranes on the PES/SPSf Substrate Through
 1688 Interfacial Polymerization. *AIChE Journal* 59, 215–228. <https://doi.org/10.1002/aic>

1689 Qin, J.J., Lay, W.C.L., Kekre, K.A., 2012. Recent developments and future challenges of
 1690 forward osmosis for desalination: A review. *Desalination and Water Treatment* 39, 123–
 1691 136. <https://doi.org/10.1080/19443994.2012.669167>

1692 Ramon, G.Z., Hoek, E.M.V., 2013. Transport through composite membranes, part 2: Impacts
 1693 of roughness on permeability and fouling. *Journal of Membrane Science* 425–426, 141–
 1694 148. <https://doi.org/10.1016/j.memsci.2012.08.004>

1695 Ramon, G.Z., Wong, M.C.Y., Hoek, E.M.V., 2012. Transport through composite membrane,
 1696 Part 1: Is there an optimal support membrane? *Journal of Membrane Science* 415–416,
 1697 298–305. <https://doi.org/10.1016/j.memsci.2012.05.013>

1698 Razmjou, A., Liu, Q., Simon, G.P., Wang, H., 2013. Bifunctional polymer hydrogel layers as

1699 forward osmosis draw agents for continuous production of fresh water using solar
 1700 energy. *Environmental Science and Technology* 47, 13160–13166.
 1701 <https://doi.org/10.1021/es403266y>

1702 Ren, J., McCutcheon, J.R., 2014. A new commercial thin film composite membrane for
 1703 forward osmosis. *Desalination* 343, 187–193.
 1704 <https://doi.org/10.1016/j.desal.2013.11.026>

1705 Roach, J.D., Al-Abdulmalek, A., Al-Naama, A., Haji, M., 2014. Use of micellar solutions as
 1706 draw agents in forward osmosis. *Journal of Surfactants and Detergents* 17, 1241–1248.
 1707 <https://doi.org/10.1007/s11743-014-1638-6>

1708 Rodríguez-Alegre, R., Zapata-Jiménez, J., You, X., Pérez-Moya, M., Sanchis, S., García-
 1709 Montaña, J., 2023. Nutrient recovery and valorisation from pig slurry liquid fraction
 1710 with membrane technologies. *Science of the Total Environment* 874.
 1711 <https://doi.org/10.1016/j.scitotenv.2023.162548>

1712 Roy, D., Rahni, M., Pierre, P., Yargeau, V., 2016. Forward osmosis for the concentration and
 1713 reuse of process saline wastewater. *Chemical Engineering Journal* 287, 277–284.
 1714 <https://doi.org/10.1016/j.cej.2015.11.012>

1715 Sahebi, S., Phuntsho, S., Eun Kim, J., Hong, S., Kyong Shon, H., 2015. Pressure assisted
 1716 fertiliser drawn osmosis process to enhance final dilution of the fertiliser draw solution
 1717 beyond osmotic equilibrium. *Journal of Membrane Science* 481, 63–72.
 1718 <https://doi.org/10.1016/j.memsci.2015.01.055>

1719 Salehi, H., Rastgar, M., Shakeri, A., 2017. Anti-fouling and high water permeable forward
 1720 osmosis membrane fabricated via layer by layer assembly of chitosan/graphene oxide.
 1721 *Applied Surface Science* 413, 99–108. <https://doi.org/10.1016/j.apsusc.2017.03.271>

1722 Sbardella, L., Blandin, G., Fàbregas, A., Carlos Real Real, J., Serra Clusellas, A., Ferrari, F.,
 1723 Bosch, C., Martinez-Lladó, X., 2022. Optimization of pilot scale forward osmosis
 1724 process integrated with electrodialysis to concentrate landfill leachate. Chemical
 1725 Engineering Journal 434. <https://doi.org/10.1016/j.cej.2021.134448>
 1726 Seyedpour, S.F., Rahimpour, A., Shamsabadi, A.A., Soroush, M., 2018. Improved
 1727 performance and antifouling properties of thin-film composite polyamide membranes
 1728 modified with nano-sized bactericidal graphene quantum dots for forward osmosis.
 1729 Chemical Engineering Research and Design 139, 321–334.
 1730 <https://doi.org/10.1016/j.cherd.2018.09.041>
 1731 Shadravan, A., Amani, M., 2021. Recent Advances of Nanomaterials in Membranes for
 1732 Osmotic Energy Harvesting by Pressure Retarded Osmosis. International Journal of
 1733 Engineering and Applied Sciences (IJEAS) 8, 1–7. <https://doi.org/10.31873/ijeas.8.8.02>
 1734 Shaffer, D.L., Jaramillo, H., Romero-Vargas Castrillón, S., Lu, X., Elimelech, M., 2015.
 1735 Post-fabrication modification of forward osmosis membranes with a poly(ethylene
 1736 glycol) block copolymer for improved organic fouling resistance. Journal of Membrane
 1737 Science 490, 209–219. <https://doi.org/10.1016/j.memsci.2015.04.060>
 1738 Shang, M., Shi, B., 2018. Study on preparation and performances of cellulose acetate forward
 1739 osmosis membrane. Chemical Papers 72, 3159–3167. [https://doi.org/10.1007/s11696-](https://doi.org/10.1007/s11696-018-0554-z)
 1740 [018-0554-z](https://doi.org/10.1007/s11696-018-0554-z)
 1741 Sharif, A., ARYAFAR, M., 2015. FO.pdf.
 1742 Shibuya, M., Park, M.J., Lim, S., Phuntsho, S., Matsuyama, H., Shon, H.K., 2018. Novel
 1743 CA/PVDF nanofiber supports strategically designed via coaxial electrospinning for high
 1744 performance thin-film composite forward osmosis membranes for desalination.
 1745 Desalination 445, 63–74. <https://doi.org/10.1016/j.desal.2018.07.025>

1746 Shokrgozar Eslah, S., Shokrollahzadeh, S., Moini Jazani, O., Samimi, A., 2018. Forward
 1747 osmosis water desalination: Fabrication of graphene oxide-polyamide/polysulfone thin-
 1748 film nanocomposite membrane with high water flux and low reverse salt diffusion.
 1749 Separation Science and Technology (Philadelphia) 53, 573–583.
 1750 <https://doi.org/10.1080/01496395.2017.1398261>

1751 Shokrollahzadeh, S., Tajik, S., 2018. Fabrication of thin film composite forward osmosis
 1752 membrane using electrospun polysulfone/polyacrylonitrile blend nanofibers as porous
 1753 substrate. Desalination 425, 68–76. <https://doi.org/10.1016/j.desal.2017.10.017>

1754 Shoorangiz, L., Karimi-Jashni, A., Azadi, F., Zerafat, M.M., 2022. Water treatment by
 1755 forward osmosis using novel D-Xylose coated magnetic nanoparticles as draw agent.
 1756 Environmental Technology (United Kingdom) 43, 3309–3318.
 1757 <https://doi.org/10.1080/09593330.2021.1921049>

1758 Song, H. ming, Zhu, L. jing, Zeng, Z. xiang, Xue, Q. ji, 2018. High performance forward
 1759 osmosis cellulose acetate (CA) membrane modified by polyvinyl alcohol and
 1760 polydopamine. Journal of Polymer Research 25. [https://doi.org/10.1007/s10965-018-](https://doi.org/10.1007/s10965-018-1555-x)
 1761 [1555-x](https://doi.org/10.1007/s10965-018-1555-x)

1762 Song, X., Liu, Z., Sun, D.D., 2011. Nano gives the answer: Breaking the bottleneck of
 1763 internal concentration polarization with a nanofiber composite forward osmosis
 1764 membrane for a high water production rate. Advanced Materials 23, 3256–3260.
 1765 <https://doi.org/10.1002/adma.201100510>

1766 Song, X., Wang, L., Tang, C.Y., Wang, Z., Gao, C., 2015. Fabrication of carbon nanotubes
 1767 incorporated double-skinned thin film nanocomposite membranes for enhanced
 1768 separation performance and antifouling capability in forward osmosis process.
 1769 Desalination 369, 1–9. <https://doi.org/10.1016/j.desal.2015.04.020>

- 1770 Stone, M.L., Rae, C., Stewart, F.F., Wilson, A.D., 2013. Switchable polarity solvents as draw
1771 solutes for forward osmosis. *DES* 312, 124–129.
1772 <https://doi.org/10.1016/j.desal.2012.07.034>
- 1773 Su, J., Yang, Q., Teo, J.F., Chung, T.S., 2010. Cellulose acetate nanofiltration hollow fiber
1774 membranes for forward osmosis processes. *Journal of Membrane Science* 355, 36–44.
1775 <https://doi.org/10.1016/j.memsci.2010.03.003>
- 1776 Suwaileh, W., Pathak, N., Shon, H., Hilal, N., 2020. Forward osmosis membranes and
1777 processes: A comprehensive review of research trends and future outlook. *Desalination*
1778 485, 114455. <https://doi.org/10.1016/j.desal.2020.114455>
- 1779 Suwaileh, W.A., Johnson, D.J., Sarp, S., Hilal, N., 2018. Advances in forward osmosis
1780 membranes: Altering the sub-layer structure via recent fabrication and chemical
1781 modification approaches. *Desalination* 436, 176–201.
1782 <https://doi.org/10.1016/j.desal.2018.01.035>
- 1783 Suzaimi, N.D., Goh, P.S., Ismail, A.F., Mamah, S.C., Malek, N.A.N.N., Lim, J.W., Wong,
1784 K.C., Hilal, N., 2020. Strategies in forward osmosis membrane substrate fabrication and
1785 modification: A review. *Membranes* 10, 1–42.
1786 <https://doi.org/10.3390/membranes10110332>
- 1787 Tavakol, I., Hadadpour, S., Shabani, Z., Ahmadzadeh Tofighy, M., Mohammadi, T., Sahebi,
1788 S., 2020. Synthesis of novel thin film composite (TFC) forward osmosis (FO)
1789 membranes incorporated with carboxylated carbon nanofibers (CNFs). *Journal of*
1790 *Environmental Chemical Engineering* 8, 104614.
1791 <https://doi.org/10.1016/j.jece.2020.104614>
- 1792 Tayel, A., Nasr, P., Sewilam, H., 2020. Enhanced water flux using uncoated magnetic
1793 nanoparticles as a draw solution in forward osmosis desalination. *Desalination and*

1794 Water Treatment 193, 169–176. <https://doi.org/10.5004/dwt.2020.25827>

1795 Tayel, A., Nasr, P., Sewilam, H., 2019. Forward osmosis desalination using pectin-coated
 1796 magnetic nanoparticles as a draw solution. *Clean Technologies and Environmental*
 1797 *Policy* 21, 1617–1628. <https://doi.org/10.1007/s10098-019-01738-5>

1798 Thabit, M.S., Hawari, A.H., Ammar, M.H., Zaidi, S., Zaragoza, G., Altaee, A., 2019.
 1799 Evaluation of forward osmosis as a pretreatment process for multi stage flash seawater
 1800 desalination. *Desalination* 461, 22–29. <https://doi.org/10.1016/j.desal.2019.03.015>

1801 Thompson, N.A., Nicoll, P.G., 2011. Forward osmosis desalination: a commercial reality.
 1802 IDA World Congress - Perth Convention and Exhibition Centre (PCEC), Perth, Western
 1803 Australia. September 4-9, 2011 16.

1804 Wang, K.Y., Ong, R.C., Chung, T.S., 2010. Double-skinned forward osmosis membranes for
 1805 reducing internal concentration polarization within the porous sublayer. *Industrial and*
 1806 *Engineering Chemistry Research* 49, 4824–4831. <https://doi.org/10.1021/ie901592d>

1807 Wang, L., Ma, F., Jia, J., Lei, X., Zhao, X., Liu, C., 2019. Investigation of forward osmosis
 1808 performance and anti-fouling properties of the novel hydrophilic polymer brush-grafted
 1809 TFC-type FO membranes. *Journal of Chemical Technology and Biotechnology* 94,
 1810 2198–2211. <https://doi.org/10.1002/jctb.6003>

1811 Wang, X., Ba, X., Cui, N., Ma, Z., Wang, L., Wang, Z., Gao, X., 2019. Preparation,
 1812 characterisation, and desalination performance study of cellulose acetate membranes
 1813 with MIL-53(Fe) additive. *Journal of Membrane Science* 590, 117057.
 1814 <https://doi.org/10.1016/j.memsci.2019.04.061>

1815 Wang, X., Wang, Xingzu, Xiao, P., Li, J., Tian, E., Zhao, Y., Ren, Y., 2016. High water
 1816 permeable free-standing cellulose triacetate/graphene oxide membrane with enhanced

1817 antibiofouling and mechanical properties for forward osmosis. *Colloids and Surfaces A:*
1818 *Physicochemical and Engineering Aspects* 508, 327–335.
1819 <https://doi.org/10.1016/j.colsurfa.2016.08.077>

1820 Wang, Y., Fang, Z., Zhao, S., Ng, D., Zhang, J., Xie, Z., 2018. Dopamine incorporating
1821 forward osmosis membranes with enhanced selectivity and antifouling properties. *RSC*
1822 *Advances* 8, 22469–22481. <https://doi.org/10.1039/c8ra03166e>

1823 Wang, Y., Yu, H., Xie, R., Zhao, K., Ju, X., Wang, W., Liu, Z., Chu, L., 2016. An easily
1824 recoverable thermo-sensitive polyelectrolyte as draw agent for forward osmosis process.
1825 *Chinese Journal of Chemical Engineering* 24, 86–93.
1826 <https://doi.org/10.1016/j.cjche.2015.11.015>

1827 Wang, Z., Tang, J., Zhu, C., Dong, Y., Wang, Q., Wu, Z., 2015. Chemical cleaning protocols
1828 for thin film composite (TFC) polyamide forward osmosis membranes used for
1829 municipal wastewater treatment. *Journal of Membrane Science* 475, 184–192.
1830 <https://doi.org/10.1016/j.memsci.2014.10.032>

1831 Wang, Z., Zheng, J., Tang, J., Wang, X., Wu, Z., 2016. A pilot-scale forward osmosis
1832 membrane system for concentrating low-strength municipal wastewater: Performance
1833 and implications. *Scientific Reports* 6, 1–11. <https://doi.org/10.1038/srep21653>

1834 Wei, J., Qiu, C., Tang, C.Y., Wang, R., Fane, A.G., 2011. Synthesis and characterization of
1835 flat-sheet thin film composite forward osmosis membranes. *Journal of Membrane*
1836 *Science* 372, 292–302. <https://doi.org/10.1016/j.memsci.2011.02.013>

1837 Wendt, D.S., Orme, C.J., Mines, G.L., Wilson, A.D., 2015. Energy requirements of the
1838 switchable polarity solvent forward osmosis (SPS-FO) water purification process.
1839 *Desalination* 374, 81–91. <https://doi.org/10.1016/j.desal.2015.07.012>

1840 Wu, Q.Y., Xing, X.Y., Yu, Y., Gu, L., Xu, Z.K., 2018. Novel thin film composite membranes
 1841 supported by cellulose triacetate porous substrates for high-performance forward
 1842 osmosis. *Polymer* 153, 150–160. <https://doi.org/10.1016/j.polymer.2018.08.017>

1843 Wu, W., Yu, L., Li, L., Li, Z., Kang, J., Pu, S., Chen, D., Ma, R., An, K., Liu, G., Yu, Y.,
 1844 2021. Electrospun nanofiber based forward osmosis membrane using graphene oxide as
 1845 substrate modifier for enhanced water flux and rejection performance. *Desalination* 518,
 1846 115283. <https://doi.org/10.1016/j.desal.2021.115283>

1847 Xu, S., Li, F., Su, B., Hu, M.Z., Gao, X., Gao, C., 2019. Novel graphene quantum dots
 1848 (GQDs)-incorporated thin film composite (TFC) membranes for forward osmosis (FO)
 1849 desalination. *Desalination* 219–230. <https://doi.org/10.1016/j.desal.2018.04.004>

1850 Xu, Y., Zhu, Y., Chen, Z., Zhu, J., Chen, G., 2022. A Comprehensive Review on Forward
 1851 Osmosis Water Treatment: Recent Advances and Prospects of Membranes and Draw
 1852 Solutes, *International Journal of Environmental Research and Public Health*.
 1853 <https://doi.org/10.3390/ijerph19138215>

1854 Yadav, S., Ibrar, I., Altaee, A., Samal, A.K., Ghobadi, R., Zhou, J., 2020a. Feasibility of
 1855 brackish water and landfill leachate treatment by GO/MoS₂-PVA composite
 1856 membranes. *Science of the Total Environment* 745.
 1857 <https://doi.org/10.1016/j.scitotenv.2020.141088>

1858 Yadav, S., Ibrar, I., Bakly, S., Khanafer, D., Altaee, A., Padmanaban, V.C., Samal, A.K.,
 1859 Hawari, A.H., 2020b. Organic fouling in forward osmosis: A comprehensive review.
 1860 *Water (Switzerland)* 12. <https://doi.org/10.3390/w12051505>

1861 Yadav, S., Saleem, H., Ibrar, I., Naji, O., Hawari, A.A., Alanezi, A.A., Zaidi, S.J., Altaee, A.,
 1862 Zhou, J., 2020c. Recent developments in forward osmosis membranes using carbon-
 1863 based nanomaterials. *Desalination* 482, 114375.

1864 <https://doi.org/10.1016/j.desal.2020.114375>

1865 Yip, N.Y., Tiraferri, A., Phillip, W.A., Schiffman, J.D., Hoover, L.A., Kim, Y.C., Elimelech,
1866 M., 2011. Thin-film composite pressure retarded osmosis membranes for sustainable
1867 power generation from salinity gradients. *Environmental Science and Technology* 45,
1868 4360–4369. <https://doi.org/10.1021/es104325z>

1869 Yu, Youngbeom, Lee, S., Maeng, S.K., 2017. Forward osmosis membrane fouling and
1870 cleaning for wastewater reuse. *Journal of Water Reuse and Desalination* 7, 111–120.
1871 <https://doi.org/10.2166/wrd.2016.023>

1872 Yu, Yuan, Wu, Q.Y., Liang, H.Q., Gu, L., Xu, Z.K., 2017. Preparation and characterization
1873 of cellulose triacetate membranes via thermally induced phase separation. *Journal of*
1874 *Applied Polymer Science* 134, 1–10. <https://doi.org/10.1002/app.44454>

1875 Zhan, M., Kim, Y., Lim, J., Hong, S., 2021. Application of fouling index for forward osmosis
1876 hybrid system: A pilot demonstration. *Journal of Membrane Science* 617, 118624.
1877 <https://doi.org/10.1016/j.memsci.2020.118624>

1878 Zhang, M., She, Q., Yan, X., Tang, C.Y., 2017. Effect of reverse solute diffusion on scaling
1879 in forward osmosis: A new control strategy by tailoring draw solution chemistry.
1880 *Desalination* 401, 230–237. <https://doi.org/10.1016/j.desal.2016.08.014>

1881 Zhang, S., Wang, K.Y., Chung, T.S., Chen, H., Jean, Y.C., Amy, G., 2010. Well-constructed
1882 cellulose acetate membranes for forward osmosis: Minimized internal concentration
1883 polarization with an ultra-thin selective layer. *Journal of Membrane Science* 360, 522–
1884 535. <https://doi.org/10.1016/j.memsci.2010.05.056>

1885 Zhao, D., Chen, S., Guo, C.X., Zhao, Q., Lu, X., 2016. Multi-functional forward osmosis
1886 draw solutes for seawater desalination. *Chinese Journal of Chemical Engineering* 24,

1887 23–30. <https://doi.org/10.1016/j.cjche.2015.06.018>

1888 Zhao, D., Chen, S., Wang, P., Zhao, Q., Lu, X., 2014a. A dendrimer-based forward osmosis
 1889 draw solute for seawater desalination. *Industrial and Engineering Chemistry Research*
 1890 53, 16170–16175. <https://doi.org/10.1021/ie5031997>

1891 Zhao, D., Wang, P., Zhao, Q., Chen, N., Lu, X., 2014b. Thermoresponsive copolymer-based
 1892 draw solution for seawater desalination in a combined process of forward osmosis and
 1893 membrane distillation. *Desalination* 348, 26–32.
 1894 <https://doi.org/10.1016/j.desal.2014.06.009>

1895 Zhao, S., Zou, L., Tang, C.Y., Mulcahy, D., 2012. Recent developments in forward osmosis:
 1896 Opportunities and challenges. *Journal of Membrane Science* 396, 1–21.
 1897 <https://doi.org/10.1016/j.memsci.2011.12.023>

1898 Zheng, K., Zhou, S., 2019. Fabrication of a novel cyanoethyl cellulose substrate for thin-film
 1899 composite forward osmosis membrane. *Blue-Green Systems* 1, 18–32.
 1900 <https://doi.org/10.2166/bgs.2019.198>

1901 Zheng, K., Zhou, S., Cheng, Z., Huang, G., 2021. Thin-film composite forward osmosis
 1902 membrane prepared from polyvinyl chloride/cellulose carbamate substrate and its
 1903 potential application in brackish water desalination. *Journal of Applied Polymer Science*
 1904 138, 1–10. <https://doi.org/10.1002/app.49939>

1905 Zhong, Y., Feng, X., Chen, W., Wang, X., Huang, K.W., Gnanou, Y., Lai, Z., 2016. Using
 1906 UCST Ionic Liquid as a Draw Solute in Forward Osmosis to Treat High-Salinity Water.
 1907 *Environmental Science and Technology* 50, 1039–1045.
 1908 <https://doi.org/10.1021/acs.est.5b03747>

1909 Zhou, A., Luo, H., Wang, Q., Chen, L., Zhang, T.C., Tao, T., 2015. Magnetic

1910 thermoresponsive ionic nanogels as novel draw agents in forward osmosis. RSC
 1911 Advances 5, 15359–15365. <https://doi.org/10.1039/c4ra12102c>

1912 Zirehpour, A., Rahimpour, A., Seyedpour, F., Jahanshahi, M., 2015. Developing new
 1913 CTA/CA-based membrane containing hydrophilic nanoparticles to enhance the forward
 1914 osmosis desalination. Desalination 371, 46–57.
 1915 <https://doi.org/10.1016/j.desal.2015.05.026>

1916 Zou, S., He, Z., 2016. Enhancing wastewater reuse by forward osmosis with self-diluted
 1917 commercial fertilizers as draw solutes. Water Research 99, 235–243.
 1918 <https://doi.org/10.1016/j.watres.2016.04.067>

1919